"STUDY THE TEMPERATURE-DEPENDENT MODELING FOR PERFORMANCE OPTIMIZATION OF MULTILAYER GRAPHENE NANORIBBON (MLGNR) BASED VLSI INTERCONNECTS"

Thesis Submitted towards the partial fulfillment for the Degree of

Master of Technology

In

VLSI Design

Submitted By:

Shubham Arora

Roll No. 601461027

Under the supervision of:

Dr. Mayank Kumar Rai

Assistant Professor

Department of Electronics & Communication Engineering

Thapar University, Patiala-147004 (Punjab)

June-2016

CERTIFICATE

I hereby declare that the work which is being presented in the thesis entitled, **"Study the Temperature-Dependent Modeling for Performance Optimization of Multilayer Graphene Nanoribbon (MLGNR) Based VLSI Interconnects"** in partial fulfillment of the requirements for the award of degree of Master of Technology in VLSI Design at Electronics and Communication Department of Thapar University, Patiala is an authentic record of my study carried out under the supervision of **Dr. Mayank Kumar Rai**, Assistant Professor, ECED.

The matter presented in this thesis has not been submitted for the award of any other degree of this or any other university.

Shubham Arora

Date: 13-07-16 **Shubham Arora**

Place: Patiala **Roll No. 601461027**

It is certified that the above statement made by the student is correct to the best of my knowledge and belief.

Mayank Kumar Rai

Date: 13-07-16 **Dr. Mayank Kumar Rai**

Place: Patiala **Assistant Professor, ECED**

Thapar University, Patiala

Counter signed by:

Dr. Sanjay Sharma **Dr. S. S. Bhatia**

Professor & Head, ECED **Dean of Academy Affairs**

Thapar University, Patiala **Thapar University, Patiala**

i

ACKNOWLEDGEMENT

It is my proud privilege to acknowledge and extend my gratitude to several people who helped me directly or indirectly in completion of this report. I express my heart full indebtedness and owe a deep sense of gratitude to my teacher and my faculty guide **Dr. Mayank Kumar Rai, Assistant Professor, Electronics and Communication Engineering Department,** for their sincere guidance and support with encouragement to go ahead.

I am also thankful to **Dr. Sanjay Sharma, Professor and Head**, **Electronics and Communication Engineering Department**, for providing us with the adequate infrastructure for carrying out the work. I am also thankful to **Dr. Amit Kohli, P.G. Coordinator, Electronics and Communication Engineering Department**, for the motivation and inspiration that triggered me for the work.

My greatest thanks to all who wished me success especially my parents. I would like to thank my friends who were always there to help me.

The study has indeed helped me to explore knowledge and avenues related to my topic and I am sure it will help me in my future.

(Shubham Arora)

ABSTRACT

The accurate performance of on-chip interconnects plays an important role to optimize the performance of integrated circuits (ICs) in deep sub-micron (DSM) technology nodes. Due to technology scaling, there has been a significant reduction in dimension size. Hence, problems of the mean free path for electrons, surface scattering from the boundaries of ultra-narrow conductors as well as grain boundary scattering inhibit electronic conduction in the copper wires to an unacceptable level. Due to technology scaling, thermal issues have also become a major challenging factor in the possible usage of on chip interconnect material for designing high performance integrated circuits. Consequently, alternative solutions such as graphene nano-ribbon (GNR) interconnects have been proposed in order to avoid the problems associated with global on-chip wires altogether.

This thesis work includes the thermally aware circuit modeling and performance analysis of multilayer graphene nano-ribbon (MLGNR) based VLSI interconnects. The temperature-dependent performance in terms of propagation delay, power dissipation and crosstalk-induced voltage noise waveform at the far end of victim line, of MLGNR interconnects, have been analyzed at 22-nm technology node. SPICE simulations using PTM level 54 model were carried out to validate the findings. The results obtained through simulation are compared with conventionally used copper interconnects and it is observed that MLGNR outperforms its counterpart at different lengths of interconnects ranging from 200μm to 1000μm over a temperature range of 300K to 500K.

A comparative performance analysis between MLGNR interconnects with resistance estimated using thermally aware model and temperature independent model (conventional) is investigated. Average relative improvements of 37.24% and 26.34% in propagation delay and power dissipation respectively are achieved using a thermally aware model in comparison with a temperature independent model of MLGNR resistance, with length variations from 200μm to 1000μm. Further, an average relative improvement in the time duration reduction of victim output, for the same range of interconnect lengths, is achieved about 35% by using a thermally aware model instead

of a temperature independent model of MLGNR resistance. Obtained results reflect that the thermally aware modeling of MLGNR is important for its performance optimization in DSM technology nodes. After the temperature-dependent comparative performance analysis, MLGNR comes out as promising alternative to copper for the use as future VLSI interconnects, due to its less sensitivity with temperature dependent scattering.

TABLE OF CONTENTS

PAGE NO.

CERTIFICATE i

ACKNOWLEDGEMENT ii

ABSTRACT iii

LIST OF ACRONYMS viii

LIST OF FIGURES ix

LIST OF TABLES xii

LIST OF SYMBOLS xiii

CHAPTER 1: INTRODUCTION AND STATEMENT OF THE PROBLEMS 1

1.1 Interconnects 1

1.1.1 Types of interconnects 1

1.1.2 Why we need carbon based interconnects 2

1.2 Graphene nano-ribbon 4

1.2.1 Basic properties of GNRs 4

1.2.2 Issues with GNR 4

1.2.3 Types of GNRs on the bases of chirality 5

1.2.4 GNR as VLSI Interconnects 6

1.3 Statement of the problems 6

1.4 Organization of thesis 7

CHAPTER 2: PERFORMANCE ANALYSIS - A REVIEW 8

2.1 Introduction 8

2.2 Literature review 8

2.3 Conclusion 13

CHAPTER 3: TEMPERATURE DEPENDENT CIRCUIT MODELING OF MLGNR INTERCONNECTS 15

3.1 Introduction 15

3.2 Temperature dependent and independent modeling of MLGNR 15

3.2.1 Temperature based resistance modeling of MLGNR 16

3.2.2 Conductance modeling of MLGNR 20

3.2.3 Inductance modeling of MLGNR 21

3.3 RLC modeling of copper based interconnects 21

3.4 Conclusion 22

CHAPTER 4: THERMALLY AWARE IMPEDANCE ANALYSIS OF MLGNR INTERCONNECTS 23

4.1 Introduction 23

4.2 Impedance analysis of MLGNR and copper interconnects 23

4.3 Conclusion 28

CHAPTER 5: THERMALLY AWARE PERFORMANCE ANALYSIS OF MLGNR INTERCONNECTS 29

5.1 Introduction 29

5.2 Temperature dependent and independent performance analysis of MLGNR 29

5.2.1 Delay and power analysis 30

5.2.1.1 Delay analysis 30

5.2.1.2 Power dissipation analysis 32

5.2.2 Crosstalk analysis 34

5.3 Conclusion 37

CHAPTER 6: A COMPARATIVE ANALYSIS BETWEEN MLGNR AND COPPER INTERCONNECTS 38

6.1 Introduction 38

6.2 Performance analysis of copper based interconnects 38

6.2.1 Delay analysis of copper 38

6.2.2 Power analysis of copper 39

6.2.3 Crosstalk analysis of copper 40

6.3 Results and comparative analysis 40

6.3.1 Comparative delay and power analysis 41

6.3.2 Comparative crosstalk analysis 43

6.4 Conclusion 45

CHAPTER 7: CONCLUDING REMARKS AND FUTURE SCOPE 46

7.1 Introduction 46

7.2 Summary of important findings 46

7.3 Suggestions for future work 48

REFERENCES 49

LIST OF PUBLICATIONS 53

ORIGINALITY REPORT

LIST OF ACRONYMS

ac-GNR	Armchair Graphene Nano-ribbon
CNT	Carbon Nanotube
CMOS	Complementary Metal Oxide Semiconductor
DSM	Deep Sub-Micron
EDP	Energy Delay Product
ESC	Equivalent Single Conductor
GHz	Giga Hertz
GNR	Graphene Nano-ribbon
IC	Integrated Circuit
ITRS	International Technology Roadmap for Semiconductor
MFP	Mean Free Path
MCB	Mixed Carbon-nanotube Bundle
MWCNT	Multi Walled Carbon Nanotube
MLGNR	Multi-Layer Graphene Nano-ribbon
PDP	Power Delay Product
RLC	Resistance-Inductance-Capacitance
SC-MLGNR	Side Contact Multi-Layer Graphene Nano-ribbon
SPICE	Simulation Program with Integrated Circuit Emphasis
SWCNT	Single Walled Carbon Nanotube
SLGNR	Single-Layer Graphene Nano-ribbon
TC-MLGNR	Top Contact Multi-Layer Graphene Nano-ribbon
VLSI	Very Large Scale Integration
zz-GNR	Zigzag Graphene Nano-ribbon

LIST OF FIGURES

		PAGE NO.
Fig. 1.1:	Cross-Section of stacked interconnects	2
Fig. 1.2:	Lattice structure of a) Graphene b) Carbon nanotube (SWCNT, MWCNT) c) Single layer GNR (SLGNR) d) Multilayer GNR (MLGNR)	5
Fig. 1.3:	a) Armchair chirality GNR b) Zigzag chirality GNR	6
Fig. 2.1:	Resistance per unit length for Cu, SWCNT-bundle, MLGNR interconnects	9
Fig. 2.2:	RLC delay ratio w.r.t. copper wire for global interconnects	10
Fig. 2.3:	Delay comparison between optical interconnects and GNR interconnects	12
Fig. 3.1:	Geometry of MLGNR interconnects	16
Fig. 3.2:	ESC equivalent model of MLGNR interconnect.	16
Fig. 3.3:	Structure of zigzag GNR	17
Fig. 3.4:	Resistive network for (a) TC-MLGNR and (b) SC-MLGNR.	19
Fig. 4.1:	Mean free path as a function of temperature.	24
Fig. 4.2:	Resistance of MLGNR interconnects as a function of temperature for different lengths.	25
Fig. 4.3:	Resistance of copper interconnects as a function of temperature for different lengths.	25
Fig. 4.4:	Resistance of MLGNR and copper based interconnects at different temperatures for 1mm long interconnects.	26
Fig. 4.5:	Resistance of thermally aware and temperature independent model of MLGNR at different lengths of interconnects.	26
Fig. 4.6:	Capacitance of MLGNR and copper interconnects w.r.t. length of interconnects.	27
Fig. 4.7:	Inductance of MLGNR and copper interconnects w.r.t. length of interconnects.	27

Fig. 5.1:	CMOS inverter driven distributed interconnect with load	30
Fig. 5.2:	Schematic of a CMOS inverter driving a global interconnect in S-Edit of Tanner EDA.	30
Fig. 5.3:	Propagation delay of MLGNR w.r.t. temperature	31
Fig. 5.4:	Propagation delay of MLGNR for temperature dependent and independent resistance models at different lengths.	31
Fig. 5.5:	Power dissipation of MLGNR w.r.t. temperature	32
Fig. 5.6:	Power Dissipation of MLGNR for temperature dependent and independent resistance models at different lengths	33
Fig. 5.7:	Capacitively coupled distributed circuit to model crosstalk between adjacent nets [36].	35
Fig. 5.8:	Thermally aware Crosstalk induced transient response of capacitively coupled interconnects for MLGNR at victim far end.	35
Fig. 5.9:	Normalized time duration as a function of interconnect length of victim output.	36
Fig. 6.1:	Propagation delay of copper interconnects w.r.t. temperature at different lengths.	39
Fig. 6.2:	Power dissipation of copper interconnects w.r.t. temperature at different lengths.	39
Fig. 6.3:	Thermally aware crosstalk induced transient response of capacitively coupled interconnects for copper at victim far end.	40
Fig. 6.4:	Delay ratio with varying temperature for long interconnect (*1mm*) at 22nm technology node.	41
Fig. 6.5:	Power ratio with varying temperature for 1mm long interconnects at 22nm technology node.	42
Fig. 6.6:	Relative percentage change in resistance w.r.t. copper for 1mm long interconnects.	42

Fig. 6.7:	Variation of normalized crosstalk induced positive noise voltage peak with temperature at the far end of the victim line.	43
Fig. 6.8:	Normalized time duration of the victim output waveform for both MLGNR and copper.	44
Fig. 6.9:	Crosstalk induced delay ratio with varying temperature for 1mm long interconnect at 22nm technology node.	45

LIST OF TABLES

		PAGE NO.
Table 1.1:	Properties of Cu, SWCNT, MWCNT and GNR	4
Table 4.1:	Simulation Parameters-ITRS 2012	24
Table 4.2:	Impedance parameters of *1mm* global interconnect: Temperature=*300K*, Technology-*22nm*	28
Table 5.1:	Average relative improvement in delay	32
Table 5.2:	Average relative improvement in power dissipation	34
Table 5.3:	Average improvement in accuracy of coupled victim output pulse width estimation using thermally aware model in comparison of temperature dependent model	36

LIST OF SYMBOLS

A	Area of cross-section
AsF_5	Arsenic penta-Fluoride
K_b	Boltzmann's constant
ρ_c	C-axis resistivity
R_c	Contact resistance
Cu	Copper
C_c	Coupling capacitance
ε	Dielectric constant
d	Distance between ground and interconnect
$\boldsymbol{\lambda_{eff}}$	Effective mean free path of MLGNR
e	Electron charge
$\boldsymbol{C_e}$	Electrostatic capacitance
E_f	Fermi Energy
$\boldsymbol{v_f}$	Fermi velocity of electrons
C_g	Ground capacitance
L_k	Kinetic inductance
l	Length of interconnect
L_m	Magnetic inductance
$\boldsymbol{\rho_m}$	Mass density of graphene
N_{ch}	Number of conducting channels
n	Number of layers
μ_0	Permeability
h	Planck's constant
$\boldsymbol{C_q}$	Quantum capacitance
R_q	Quantum resistance
R_o	Resistance of copper at 300K
$\boldsymbol{\rho_0}$	Resistivity of copper at 300K
R_s	Scattering resistance
$\boldsymbol{L_s}$	Self-inductance
s	Separation between adjacent interconnects
T	Temperature

$\boldsymbol{\alpha}$	Temperature coefficient of resistance
t	Thickness of interconnect
T_c	Transmission coefficient
δ	Van-der waal gap
w	Width of interconnect

CHAPTER 1

INTRODUCTION AND STATEMENT OF THE PROBLEMS

1.1 Interconnects

The conducting material which provides electrical connection between two or more nodes of a system/circuit in a chip is known as a VLSI Interconnect. Interconnects provide power supply and clock to a device. Interconnects also deliver the output of one device to another device. Interconnect is a three dimensional structure which has its own resistance and capacitance. Interconnects are as important as transistors. Performance of a chip is measured on the basis of three parameters speed, power and noise. Interconnects play a major role in performance of a VLSI chip.

1.1.1 Types of Interconnects

On the basis of length and function they perform, there are basically three types of interconnects [1]:

I. Local Interconnects

Local interconnects are very thin interconnect wires and are used to connect gates and transistors within a functional block on a chip. Local interconnects usually occupy first and second metal layers.

II. Intermediate Interconnects

Intermediate interconnects provide lower resistance than local interconnects because of more width. They are taller than local interconnects. Intermediate interconnects deliver clock and signal distribution inside a functional block.

III. Global Interconnects

Global interconnects offer clock and signal distribution between the functional blocks. They also deliver power and ground to all the functions on a chip. Length of global interconnects is usually larger than both local and intermediate interconnects. They dominate the top one or two layers. Because of larger length they play a vital part

in performance of chip. Global wires should have small resistance so that voltage does not get dropped and there is no delay in clock, otherwise clock skew can occur.

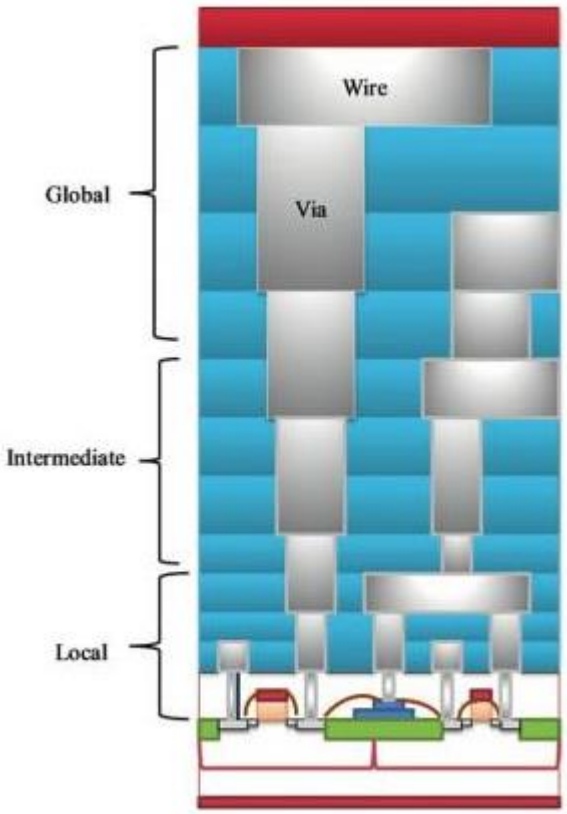

Fig. 1.1. Cross-Section of stacked interconnects [1].

1.1.2 Why we need carbon based interconnects

There has been an exponential gain in integrated circuit performance because of technology scaling. These key developments at the integrated circuit (IC) level were driven primarily by enhancement in device performance with technology scaling. With the decrease in device dimensions, there was a rapid increase in number of devices packed into a given area, which results in increasing the number of connections between these devices. An increase in the number of connections leads to a higher wiring density, thus a drop in the cross sectional dimensions of wires. Due to enhancement in the performance of devices with scaling and degradation in the performance of interconnects with scaling, interconnects have become a serious bottleneck to the performance of integrated circuits [2].

Earlier aluminium (Al) was the most commonly used material for interconnects because of its adherence on silicon dioxide and good conductivity. Additional valuable property

of Al is that it customs good ohmic contact with silicon (Si). The drawback with Al is that at high current densities considerable electro-migration takes place. Due to this limitation of aluminium, copper was introduced as interconnects. Copper is numerous times more resistant to electro migration than aluminium. Melting point of copper is higher than aluminium and thus copper is more thermally stability than aluminium. Because of the benefits it proposes Cu became the favourite interconnect material, mainly for submicron and deep submicron high density, high performance chips [3]. Due to technology scaling number of devices on same chip has increased and hence number of connections has also been increased. A significant increase in current density is seen as the outcome of dimension scaling. So, with the scaling of technology these effects on resistivity in addition to increase in interconnect resistance with length increases delay. Moreover, both propagation delay and interconnect power dissipation increases due to increase in frequency of operation and increased current density. Because of increase in power dissipation there is heating problem which assists electro-migration. So, there is a need to discover an alternative material that has superior properties than Cu and which can be used as a VLSI Interconnect [3-4, 9].

Because of their excellent physical properties, carbon based materials are suggested for future interconnect technology. Both CNT and GNR are derivatives of graphene. CNT is obtained by rolling up a graphene sheet to a hollow cylinder while GNR is obtained by patterning graphene to a thin strip. Since the carbon-carbon bond is the strongest atomic bond in nature, GNR and CNT interconnects are immune to electro-migration. Due to unique physical properties (stated in Table 1.1), such as exceptionally high current carrying capacities, thermal conductivities, large mean free path (MFP) and immunity to electro-migration carbon based interconnects can be better interconnect than copper. One main advantage of GNR over CNT is that the chirality of GNR can be controlled during the lithography and etching process, while the chirality of CNT is randomly determined by the unknown growth conditions [5-8, 10].

Table 1.1: Properties of Cu, SWCNT, MWCNT and GNR [6, 7].

	Copper	SWCNT	MWCNT	GNR
Max. Current Density (A/cm^2)	10^7	$>10^9$	$>10^9$	$>10^8$
Tensile Strength (GPa)	0.22	22.2+-2.2	11-63	-
Melting Point (K)	1356	3773 (graphite)		
Thermal Conductivity ($\times 10^3 W/mK$)	0.385	1.75-5.8	3	3-5
Mean Free Path (nm)	40	$>10^3$	2.5×10^4	1×10^3

1.2 Graphene nano-ribbon

GNRs are achieved by patterning graphene. Graphene is a flat single-layer of carbon atoms tightly packed into a 2-D honeycomb lattice (shown in Fig. 1.2) and is an elementary building block of carbon nanotubes (CNTs), GNRs, graphite, etc. [6]. Many researchers have proposed GNR as one of the promising candidate material for both transistors and interconnect.

1.2.1 Basic properties of GNRs [7]

• Large thermal conductivity ($3 - 5 \times 10^3 W/mK$)

• Large current carrying capability ($5 - 20 \times 10^8$ A/cm^2)

• High melting point (3773K (Graphite))

• Large mean free path of electrons ($1 \times 10^3 nm$)

• Small Capacitance

1.2.2 Issues with GNR

• Edge Scattering: There is a problem of edge scattering in GNRs which reduces its mean free path.

• Electron Hopping: Single layer graphene nano-ribbon (SLGNR) has large mean free path and conductivity; whereas multi-layer graphene nano-ribbon (MLGNR) turns to

graphite and has much lower conductivity per layer because of inter-sheet electron hopping [4].

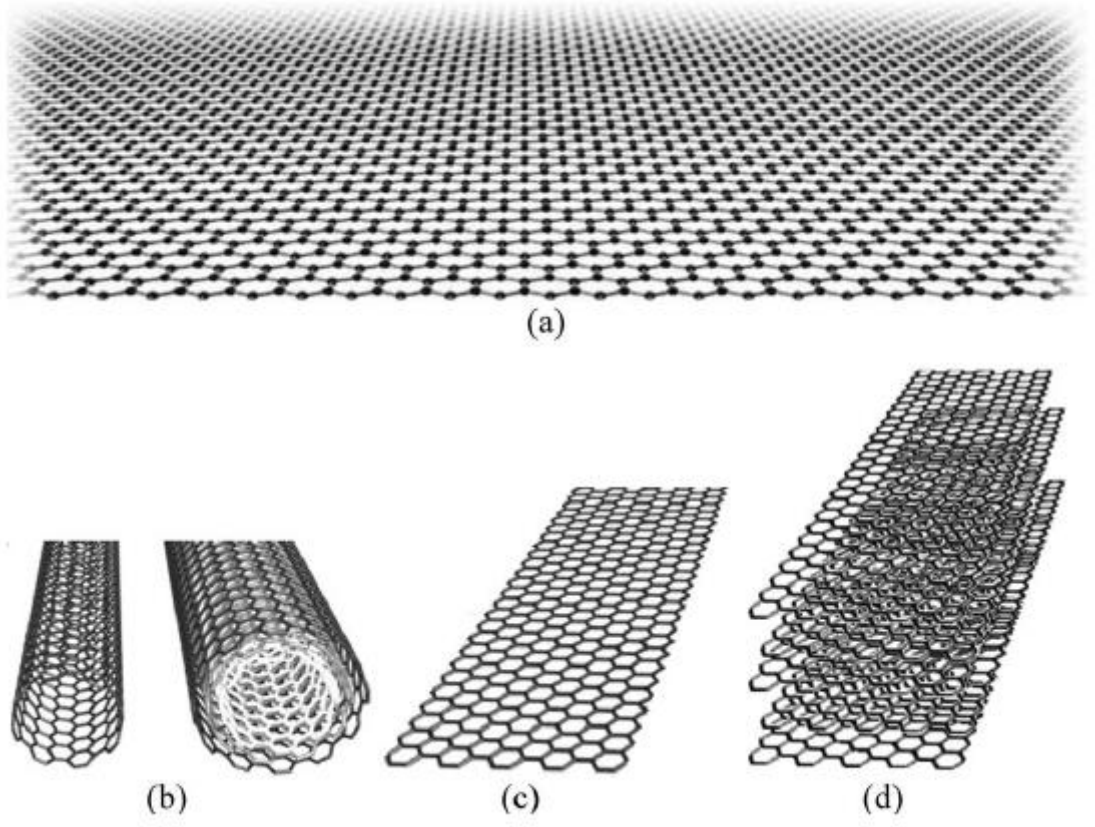

Fig. 1.2. Lattice structure of a) Graphene b) Carbon nanotube (SWCNT, MWCNT) c) Single layer GNR (SLGNR) d) Multilayer GNR (MLGNR) [6]

1.2.3 Types of GNRs on the bases of chirality

Chirality of GNRs can be controlled by fabrication processes; hence it is preferable to its counterpart CNTs. Depending upon the chirality GNR is of two types:

1. Zigzag GNR
2. Armchair GNR

GNRs can be either metallic or semiconducting according to the shape of the atomic edge as shown in Fig. 1.3. Zigzag GNRs are always metallic in nature. But, armchair GNRs are metallic if the number of atoms along the width is 3k + 2 and is

semiconducting in nature if number of atoms along the width is 3k or 3k+1, where k is an integer [6-7, 11].

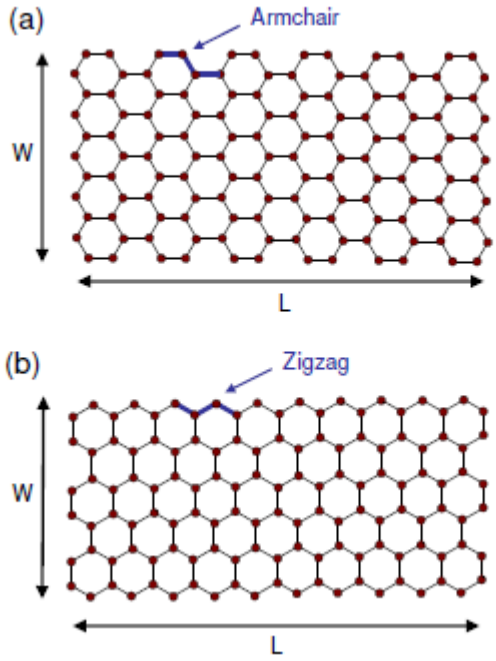

Fig. 1.3. a) Armchair chirality GNR b) Zigzag chirality GNR [11]

1.2.4 GNR as VLSI interconnects

Many researchers have proposed GNR as potential candidate material for both interconnects and transistors. GNR interconnects can be characterized as:

- Single-Layer GNR (SLGNR)
- Multi-layer GNR (MLGNR)

Single layer GNRs (SLGNR) have large mean free path, but SLGNRs can't outperform copper because of large resistance values. So, to decrease its resistance value, multiple GNR layers can be used as interconnects known as Multi-layer GNRs (MLGNR) as shown in Fig. 1.2(c, d). Further the performance of MLGNR can be improved by using intercalation doped MLGNR instead of normal MLGNR [12].

1.3 Statement of the problems

As the technology is scaling, there is a need of better interconnect material than copper. From the recent studies, it has been observed that a lot of efforts have been made from last decade to model the GNR as VLSI interconnects. Single layer GNR, Multi-layer GNR have been analysed and their equivalent RLC models have been derived. Effect of

various parameters on propagation delay and power dissipation in these interconnects have been studied. But, effects of rise in temperature on the performance of MLGNR are yet to be studied. The objectives of the proposed work are as follows:

- Development of temperature-dependent impedance parameters of MLGNR based interconnects.
- To study the effect of temperature variation on propagation delay and power dissipation in MLGNR interconnects.
- To analyse the crosstalk effects in MLGNR interconnects with variations in temperature.
- Comparison of results obtained from above analysis with results for copper interconnects at 22nm technology nodes.

1.4 Organization of thesis

Chapter 2 includes literature review of interconnect technologies; starting from the basics to the advancement towards the graphene nano-ribbon (GNR) interconnects. A brief survey of the various works that has been done by researchers is presented. Along with that, the recent research in modeling graphene nano-ribbons interconnects is presented.

Chapter 3 includes the temperature dependent circuit modeling of MLGNR based interconnects. ESC model is used for circuit modeling of MLGNR interconnects. Two different resistance models side contact and top contact are presented in this chapter.

Chapter 4 briefly introduces the basic concepts of interconnect analysis. Temperature dependent impedance parameters are given in this chapter for MLGNR and copper interconnects. A detailed thermally aware impedance analysis is presented for 22nm technology node.

Chapter 5 presents a delay model used for delay analysis of MLGNR interconnects. Thermally aware performance analysis of MLGNR in terms of propagation delay, power dissipation and crosstalk noise at different global lengths at 22nm technology node is shown in this chapter.

Chapter 6 compares the performance of MLGNR interconnects with that of copper interconnects for different temperature and at different global lengths of interconnect ranging from 200μm to 1000μm. It is found that in terms of propagation delay, power dissipation and crosstalk MLGNR gives better performance than copper interconnects.

Finally, a conclusion and future scope of the thesis is given in **Chapter 7**.

CHAPTER 2

PERFORMANCE ANALYSIS - A REVIEW

2.1 Introduction

As the technology is scaling down, device dimensions are continuously decreasing. Due to this, effect of interconnect lines on the performance of integrated circuits is becoming significant. Number of connections in a VLSI chip is increasing rapidly and hence, the cross-sectional dimensions have to be reduced. Problems of grain boundary and surface scattering are there in traditionally used copper based interconnects due to reduction in cross-sectional dimensions of interconnects. Hence, there is a need of alternative interconnect material. Carbon based interconnects with their extraordinary physical properties are being considered as a prominent interconnect material [4-10].

In this chapter works of many researchers are briefly described. Possibility of GNR based interconnects is given by different authors. Modeling and performance analysis of MLGNR interconnects done by different researchers in recent years is shown in section 2.2. Then, a brief conclusion of this chapter is given in section 2.3.

2.2 Literature review

T. Ragheb and Y. Massoud, 2008[11] gave a comprehensive resistance model for graphene nano-ribbon (GNR) interconnects. They modelled the influence of stacking of graphene layers in multi-layer GNR (MLGNR) interconnects. In this paper GNR interconnects were compared with both conventional Cu interconnects and single-walled carbon nanotube (SWCNT) bundle interconnects on the basis of resistance. Fig. 2.1 shows the comparison done by them, between the resistance of MLGNR, SWCNT and copper interconnects for different width of interconnects and it is seen that the MLGNR has lower resistance than both SWCNT and copper interconnects. They demonstrated the performance superiority of multi-layer GNR interconnects over

conventional copper interconnects at small widths (<15 nm). So, they stated that the multi-layer GNR (MLGNR) based interconnects can be used instead of copper in future as the feature size is decreasing in the VLSI industry. They observed that due to GNRs exceptional characteristics, immunity to electro-migration, ease of fabrication, and weak temperature-dependence, GNR-based technology had the potential to provide a great alternative for future interconnects.

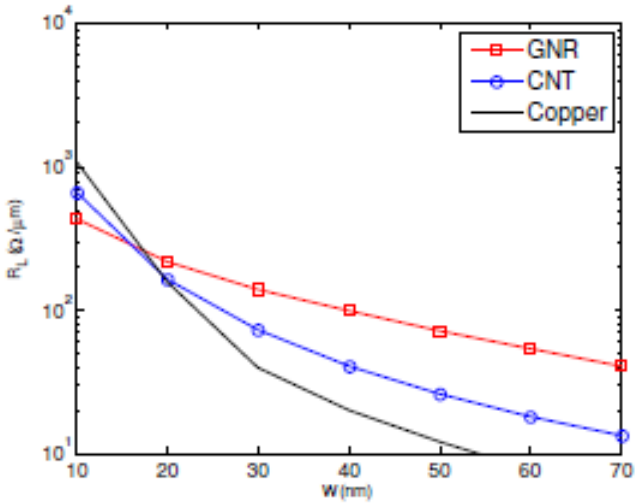

Fig. 2.1. Resistance per unit length for Cu, SWCNT-bundle, MLGNR interconnects [11]

K. Banerjee *et al.*, 2009[4] presented the delay analysis of graphene nano-ribbon interconnect. They observed the effect of edge specularity on the conductance of GNR interconnects. They also compared the performance of GNR with the Cu and CNT interconnects. Their analysis revealed that GNRs have some fabrication advantages over CNTs. But to make GNR better than its counterparts i.e. Cu and CNTs, at local as well as global levels, certain distinct technology improvements must be attained. They compared the delay of AsF_5 doped MLGNR with SWCNT interconnect as shown in Fig. 2.2. It is shown that the AsF_5 doped multilayer GNR with perfect edges have lowest delay ratio among SWCNT, SLGNR and MLGNR with rough edges. It is also revealed that very specular edges (p > 0.8) and appropriate intercalation doping are essential to make zigzag-multilayer graphene nano-ribbon (zz-MLGNR) interconnects comparable to or better than copper and carbon nanotube based interconnects at either the global or local level. They also demonstrated that intercalation-doped zz-MLGNRs can have better performance than that of tungsten (W) (even for p = 0) at local level, implying possible application as local interconnects in certain cases.

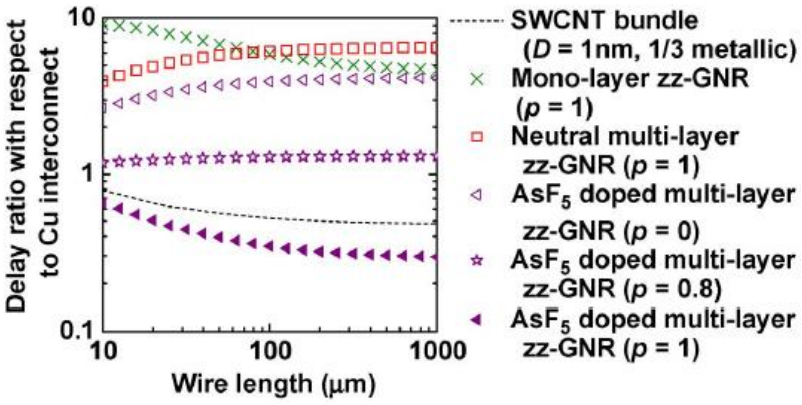

Fig. 2.2. RLC delay ratio w.r.t. copper wire for global interconnects [4]

Naeemi *et al.*, 2012[13] derived a physical model for the effective resistance of multilayer graphene nano-ribbon (MLGNR) interconnects. For the derivation of this model they considered the c-axis resistivity of MLGNR interconnects. They founded that increasing the number of layers does not essentially translate into a decrease in the overall resistance of MLGNR interconnects. They observed that there is a saturation point for effective resistance while increasing the number of layers. They evaluated the optimal number of layers to minimize the propagation delay and the energy–delay product of MLGNR interconnects. It is found that the optimal number of layers depends on the interconnect length, interlayer resistance, and the kind of contact that is used. Their comparison shows that the delay of MLGNR is lower than that of copper interconnects, if the GNR edges are smooth and if minimum-sized drivers are used. The propagation delay of MLGNR based interconnects with side contact is higher than that of Cu interconnects, if the graphene nano-ribbon edges are rough. Considering Fermi energy (E_f) = 0.2 eV, they found that the energy delay product (EDP) of MLGNR interconnects with perfect edges (smooth edges) is lower than that of Cu based interconnects.

A. G. Chiariello, A. Maffucci, 2012[14] presented the performance analysis of global-level on-chip interconnects. They gave the simple circuit equivalent model for carbon nanotubes or graphene nano-ribbons. They included the size and thermal effects into the circuit models for carbon nanotube and graphene nano-ribbon interconnects. While

assuming the mean free path of GNR constant with temperature they calculated the change in number of conducting channel with the temperature. Their study demonstrated that GNR and MWCNT based interconnects were less sensitive to temperature change as compare to copper and SWCNT ones and were potential candidate to replace Cu for wiring a VLSI chip.

A. Maffucci and G. Miano, 2013 [15] modelled the signal propagation in graphene nano-ribbon (GNR) interconnects. They studied the behaviour of number of conducting channels of armchair GNRs and zigzag GNRs as width of interconnect vary. They expressed the kinetic inductance and quantum capacitance in terms of number of conducting channels. The effective number of conducting channels was evaluated according to the semi classical Boltzmann transport theory.

V. Kumar *et al.*, 2013[2] reviewed the analytical models earlier developed for multi-layer GNR (MLGNR) with top contacts. They compared the multi-conductor transmission line (MTL) models and the simplified equivalent distributed RC model for GNR. The MTL models are used to show the distribution of current among different layers along the interconnect length. They observed that the multi-conductor transmission line (MTL) models can precisely predict the frequency response of the GNR interconnects. They also derived the optimal number of GNR layers for minimization of the propagation delay and energy-delay-product (EDP) using the distributed RC models. They compared the performance of GNRs with copper interconnects and they found that for smaller interconnects lengths, multi-layer GNR (MLGNR) with perfect edges can perform better than Cu interconnects.

W. S. Zhao and W. Y. Yin, **2014[10]** investigated the transmission performance of MLGNR interconnects with top contacts and side contacts theoretically based on their ESC model. They observed that the number of conducting channels of a metallic MLGNR interconnect is linearly dependent on width and Fermi energy (E_F). They also developed the Equivalent inductance and capacitance equations for the ESC model. It was established that the top contacts in MLGNR interconnects have larger resistance in comparison with that of side-contacts for smaller lengths of interconnect. They proved

that MLGNR interconnects can provide better performance than copper interconnects in particular at semi-global level. Even with the maximum crosstalk impacts considered, the advantage of MLGNR interconnects over copper interconnects can still be retained. According to them Fermi energy and the edge roughness are two significant factors that affect the performance of MLGNR interconnect.

A. K. Nishad and R. Sharma, 2014[16] proposed the analytical time domain models for multilayer GNR (MLGNR). Their analysis was done for both top contact MLGNR and side contact MLGNR. They stated that the performance of side contact MLGNR is far better than top contact MLGNR but the fabrication of side contact MLGNR is very difficult. They optimized the top contact MLGNR to make it perform better than copper interconnect. Performance of their optimized design of top contact MLGNR matched the side contact MLGNR. They also compared the performance of top contact MLGNR with the optical interconnects and it was found that the MLGNR's performance exceeds the performance of optical interconnects in terms of delay as shown in Fig. 2.3. It can be clearly seen that for the interconnect lengths of less than 500μm MLGNR outperforms optical interconnects in terms of propagation delay.

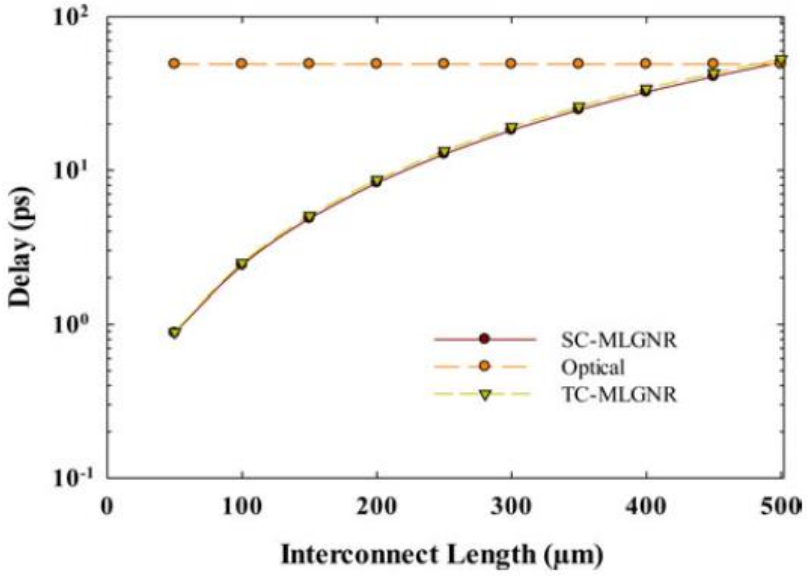

Fig. 2.3. Delay comparison between optical interconnects and GNR interconnects [16].

B. K. Kaushik *et al.*, 2015[17] analysed the performance of doped MLGNR interconnects and found that the conductivity of doped MLGNR is much higher than neutral MLGNR interconnects. Using an equivalent single conductor model they compared the doped MLGNR interconnects with the copper interconnects on the basis of power dissipation, propagation delay, and bandwidth. For similar dimensions, they found that the propagation delay and power dissipation of doped MLGNR was substantially smaller by 86.13% and 43.72%, respectively, in comparison to the copper interconnects. They witnessed that the doped MLGNR with smooth edges shows four times higher bandwidths in comparison to copper at intermediate and global interconnect lengths due to smaller parasitics. They also compared the performance of MLGNR interconnects with different edge roughness with the performance of copper interconnects. They observed a significant change in the performance of MLGNR interconnects with higher edge roughness probability.

M.K. Rai *et al.*, 2016[5] addressed the effect of interlayer resistance because of contact resistance and c-axis resistivity on performance of multi-layer graphene nano-ribbon (MLGNR) interconnects. They also observed the impact of Fermi energy on performance of MLGNR interconnects. In their analysis, they included the inductive and capacitive coupling between the adjacent layers of MLGNR. At 22nm technology node, they compared the performance of MLGNR with the copper interconnects on the basis of propagation delay, power dissipation and power delay product (PDP). It was found that for the intermediate to global interconnect lengths (300μm to 1000μm) MLGNR interconnects give much better performance than the copper interconnects. M. K. Rai *et al.* investigated that the performance gap between MLGNR with and without interlayer resistance decreases with increase in Fermi energy.

2.3 Conclusion

Resistance of MLGNR interconnects is found to be very much less than the conventionally used copper interconnects. Hence, the delay analysis shows that the MLGNR gives better delay performance than its copper counterpart. Different models to analyse the performance of GNR based interconnects are reviewed. Performance of SLGNR, MLGNR and AsF_5 doped MLGNR is analysed and for different lengths of

interconnects AsF_5 doped MLGNR has given best results. Side contact MLGNR and top contact MLGNR interconnects are studied in detail. After doing the literature survey many gaps in the study are found. No major work is done on thermally aware performance analysis of MLGNR based interconnects. A detailed crosstalk analysis of MLGNR is also needed to ensure MLGNR as a promising candidate to replace copper material.

CHAPTER 3

TEMPERATURE DEPENDENT CIRCUIT MODELING OF MLGNR INTERCONNECTS

3.1 Introduction

With advancement of VLSI technology, the number of on chip interconnects is on the rise. As the technology is scaled down, the temperature of conventionally used copper interconnects increases due to the combined effect of an increase in the resistivity of metal and current density. Thermal issues have become a key challenging factor in the possible usage of on chip interconnect material for designing high performance integrated circuits. High performance integrated circuits have a large variance in temperature. So, a better interconnect material is needed to replace copper. Carbon based interconnects with good thermal conductivity are most prominent candidates to replace copper based VLSI interconnects. MLGNR having fabrication advantage to CNT based interconnects is thus considered to be future VLSI interconnect material.

In this chapter, temperature dependent impedance parameters of MLGNR and copper interconnect at 22nm technology node are given. Depending upon the types of contact (side contact or top contact) two different resistance models of MLGNR are presented in this chapter. Temperature independent resistance model of MLGNR based interconnects is also presented.

3.2 Temperature dependent and independent modeling of MLGNR

An analytical model of MLGNR based on the geometry is presented in this section. The MLGNR is viewed as the stacked of SLGNRs as shown in Fig. 3.1. In Fig. 3.1 a MLGNR of thickness (t) and width (w) is shown placed above the ground at a distance (d). Value of the permittivity of the medium is taken as 3.25 [1].

The equivalent single conductor (ESC) model of MLGNR is a combination of ESC models of parallel SLGNRs. Initially, the simple ESC model of individual GNR is derived considering the parasitic elements like resistance, capacitance and inductance.

Later, these equivalent circuit models are combined to build up the final ESC model of MLGNR as shown in Fig. 3.2.

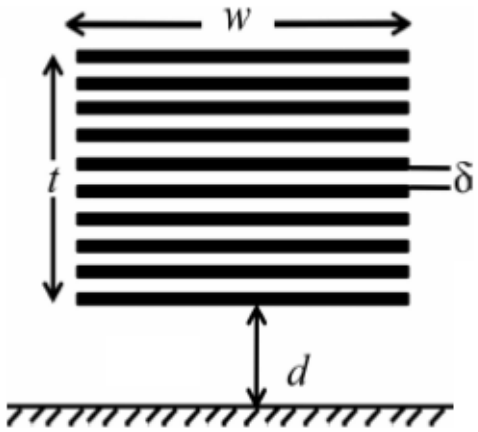

Fig. 3.1. Geometry of MLGNR interconnects [17].

n is the total number of layers in MLGNR and can be calculated [21] using Eq. (3.1)

$$n = 1 + round\left(\frac{t}{\delta}\right) \quad (3.1),$$

where, $\delta = 0.34nm$ is van-der waal gap [].

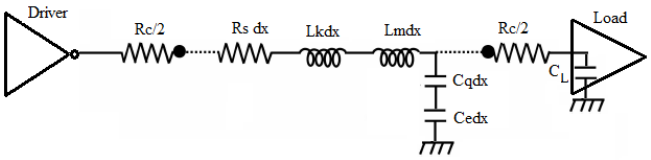

Fig. 3.2. ESC equivalent model of MLGNR interconnect.

In Fig. 3.2, dx is the differential element along the interconnect length.

3.2.1 Temperature based resistance modeling of MLGNR

In order to model the resistance of MLGNR interconnects, it is a critical need to investigate the different types and source of scattering with temperature that impact the mean free path of graphene nano-ribbons. The resistance of GNR interconnects has three components: the imperfect contact resistance (R_c) at the two ends of the GNR, the quantum resistance (R_q) and the scattering resistance (R_s).

Contact Resistance:

R_c is the imperfect contact resistance, which is highly process dependent [20] and can be approximated by Eq. (3.2) [19],

$$R_c = {}^{h}/_{(2e^2 N_{Ch} T_c)} \quad (3.2),$$

where, h is the planck's constant, e is the electron charge, n is number of layers (Eq. (1)), N_{Ch} is number of conducting channels (Eq. (3)) and T_c is the transmission coefficient and is a dimension less factor having a value less than unity [19]. The imperfect contact resistance (R_c) has a typical value ranging from *1 kΩ* to*20kΩ* **[17]**.

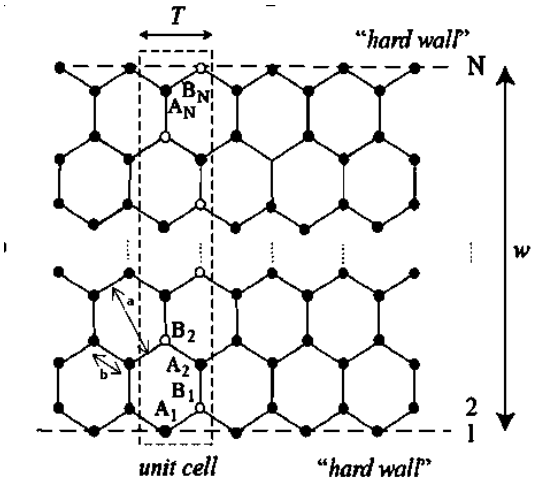

Fig. 3.3. Structure of zigzag GNR [15].

N_{ch} depends on the geometry and material and is given by following equation [22-23]:

$$N_{Ch} = \sum_{i=0}^{n_c}(1 + e^{\frac{E_i - E_f}{K_b T}})^{-1} + \sum_{i=0}^{n_v}(1 + e^{\frac{E_i + E_f}{K_b T}})^{-1} \quad (3.3),$$

where, n_c is number of conduction sub-bands, n_v is valence sub-bands. Since conduction is mainly due to electrons only. Therefore, N_{ch} is calculated by considering conduction sub-bands only. Number of sub-bands for zz-GNRs can be obtained by $n_c = \frac{2w}{\sqrt{3}a}$, a=$\sqrt{3}b$, where b is inter atomic distance [15] as shown in Fig. 3.3. E_i is the lowest (highest) energy of the ith-conduction (valence) sub-band and is given by Eq. (3.4) [10, 22],

$$E_i = \frac{h v_F}{2w}|i|, i \neq 0 \quad (3.4)$$

Fermi energy of 0.2eV is assumed for MLGNR [10].

Quantum Resistance:

R_q is the fundamental quantum resistance associated with GNR of length less than the MFP (λ_{GNR}) of electrons. For lengths less than MFP, electron transport within the nano-ribbon is essentially ballistic, and resistance is independent of length [7]. Quantum resistance is because of quantum confinement of carriers across the interconnect width.

Quantum resistance of a single layer graphene nano-ribbon can be calculated by Eq. (3.5),

$$R_q = \frac{h/_{2e^2}}{N_{Ch}} \tag{3.5}$$

Scattering Resistance:

If the GNR length (*l*) is greater than mean free path, then enhancement of scattering (due to the static impurity scattering, defects and line edge roughness scattering [24-27]), gives rise to an additional resistance. That is called scattering resistance (R_s). Since, different scattering mechanisms have different dependent parameters and scattering lengths. Thus, the effective mean free path (MFP) of MLGNR is a combined effect of all scattering lengths. MFP of MLGNR depends on many parameters, such as length, voltage bias, and temperature [7]. In this analysis, the low bias regime is considered. This is due to the fact that at higher bias where the electric field is very high, current saturates and GNR does not show ohmic behaviour. On the other hand, in the low bias regime, GNR shows perfect ohmic behaviour and are suitable for VLSI interconnect applications [28].

The scattering resistance as a function of temperature of single-layer GNR (SLGNR) interconnects per unit length is determined by Eq. (3.6) [19],

$$R_S = \frac{h}{2e^2}\frac{1}{N_{ch}.\lambda_{eff}(T)} = 12.9/(N_{ch.}\lambda_{eff}(T))\ \ k\Omega \tag{3.6}$$

It can be seen from Eq. (6) that the scattering resistance of GNR is a function of thermally-aware effective MFP (λeff).The thermally aware effective mean free path of electron in GNR is calculated by Eq. (3.7) [19],

$$\frac{1}{\lambda_{eff}(T)} = \frac{1}{\lambda^{AC}} + \frac{1}{\lambda^{op}_{abs}} + \frac{1}{\lambda^{op}_{emm}} \tag{3.7},$$

where, λ^{AC} is due to acoustic phonon scattering, $\lambda^{op}_{abs}$is due to scattering by non-polar optical phonon (absorption) and λ^{op}_{emm} is due to scattering by non-polar optical phonon(emission). MFP due to acoustic scattering is given by Eq. (3.8),

$$\lambda^{AC} = 4\frac{\rho_m(\frac{h}{2\pi}\upsilon_F\upsilon_s)^2}{\sqrt{\pi N_s}D^2_{AC}K_BT} \tag{3.8},$$

where, ρ_m is the mass density of graphene ($7.6 \times 10^{-7} kg/m^2$), υ_s is the speed of acoustic phonons(*20km/s*), υ_F is the Fermi velocity of electrons($8 \times 10^5 m/s$), N_S is the

concentration of 2-D electron gas in graphene($\cong 4 \times 10^{16}/m^2$) and D_{AC} is the acoustic deformation potential ($8eV$) [19]. MFP due to optical absorption and optical emission are given by Eqs. (3.9) and (3.10) respectively,

$$\lambda_{abs}^{op} = \frac{\rho_m \frac{h}{2\pi} w_{op} {\upsilon_F}^2}{\sqrt{\pi N_S} D_{op}^2 N_{op,abs}(1+\frac{w_{op}}{\upsilon_F \sqrt{\pi N_S}})} \quad (3.9),$$

$$\lambda_{emm}^{op} = \frac{\rho_m \frac{h}{2\pi} w_{op} {\upsilon_F}^2}{\sqrt{\pi N_S} D_{op}^2 N_{op,emm}(1-\frac{w_{op}}{\upsilon_F \sqrt{\pi N_S}})} \quad (3.10),$$

where, D_{op} is the optical deformation potential($2\times 10^{11} eV/m$) [19], $\frac{h}{2\pi} w_{op}$ is the optical phonon energy($\sim 160meV$),and N_{op} is the optical phonon number [29], and can be calculated by Eq. (3.11),

$$N_{op} = \frac{1}{e^{\frac{\frac{h}{2\pi} w_{op}}{KT}} - 1} \quad (3.11)$$

Depending upon the type of contact, MLGNR can be classified as top contact MLGNR (TC-MLGNR) and side contact MLGNR (SC-MLGNR) with connection of surrounding devices as shown in Fig. 3.4 [16].

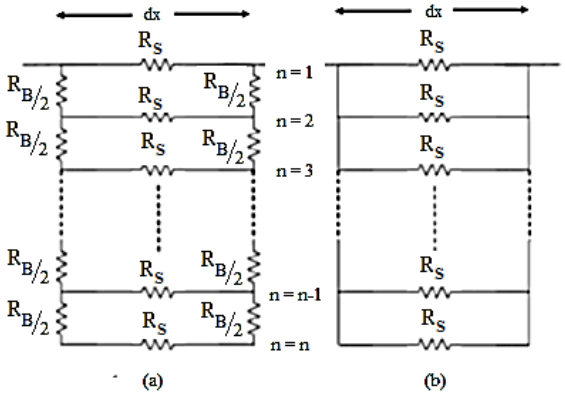

Fig. 3.4. Resistive network for (a) TC-MLGNR and (b) SC-MLGNR.

Therefore, the equivalent low bias resistance of MLGNR is different in two such cases. In case of TC-MLGNR, only the top layer is coupled with contacts. Thus, in addition to scattering resistance, an additional interlayer resistance (R_B) appears in the equivalent resistance of TC-MLGNR [16]. The equivalent resistance per unit length of TC-MLGNR is given by Eq. (3.12),

$$R_n = (\frac{1}{R_S} + \frac{1}{R_B + R_{n-1}})^{-1} \quad (3.12),$$

where, R_B is the interlayer resistance of the GNR and R_S is the scattering resistance given by Eq. (3.6) .

$$R_B = \left(\frac{\rho_c.\delta}{\Delta x.w}\right) \tag{3.13},$$

where, ρ_c is the c-axis resistivity[30], dx is the differential element along the interconnect length and w is the width of one layer.

In case of SC-MLGNR, all SLGNRs are physically connected. Therefore, for longer MLGNR ($l>\lambda_{GNR}$), the total thermally aware resistance of SC-MLGNR can be calculated by Eq. (3.14)[10, 16, 19],

$$R_{SC-MLGNR} = \frac{12.9}{n.N_{ch}}\left(1 + \frac{l}{\lambda_{eff}(T)}\right) \tag{3.14}$$

where, t is thickness of interconnect .

It can be seen from Eqs. (3.12) and (3.14) that the equivalent resistance of SC-MLGNR will always be lesser in comparison with TC-MLGNR. It indicates the desirable effect of reducing interconnect performance in terms of propagation delay, power dissipation and crosstalk. It is also reported that the SC-MLGNR has better performance in comparison with TC-MLGNR [16].This is due to the lower resistance offered by SC-MLGNR. Thus, in the present study, MLGNR has been assumed to be SC-MLGNR.

3.2.2 Conductance modeling of MLGNR

The capacitance of each GNR consists of quantum capacitance (C_q) and electrostatic capacitance (C_e) [5-6, 16].The per unit length quantum capacitance (C_q) and electrostatic capacitance (C_e) of MLGNR are given by Eqs. (3.15) and (3.16),respectively,

$$C_q = \frac{4e^2 nNch}{h\upsilon_F} \tag{3.15},$$

$$C_e = \varepsilon.M\left[tanh\left(\frac{\pi w}{4d}\right)\right] \tag{3.16}$$

The electrostatic capacitance (C_e) is calculated using conformal mapping method with width 'w', placed at a distance (d) above the ground plane [16].

$$M(a) = \begin{cases} \frac{2\pi}{ln\frac{2.(1+\sqrt[4]{1-a^2})}{(1-\sqrt[4]{1-a^2})}}, & 0 \le a < \frac{1}{\sqrt{2}} \\ \frac{2}{\pi} ln\frac{2(1+\sqrt{a})}{(1-\sqrt{a})}, & \frac{1}{\sqrt{2}} \le a \le 1 \end{cases} \tag{3.17},$$

where, 'ε' is a permittivity of the medium and 'a' is the hyperbolic tangent of function of width 'w' and distance 'y' above the ground plane.

3.2.3 Inductance modeling of MLGNR

GNR has kinetic inductance (L_k) in addition to magnetic inductance (L_m) [5, 10, 16].The kinetic inductance (L_k) is the kinetic energy stored in each conducting channel of the GNR. The magnetic inductance (L_m) captures the influence of the voltage induced by magnetic fields produced by time varying currents which is summarized in Ampere's Faraday's laws and dependent on the whole current loop. The per unit length L_k and L_m of MLGNR are given by Eqs. (3.18) and (3.19) respectively,

$$L_k = \frac{h}{4e^2 v_f n N_{ch}} \tag{3.18},$$

$$L_m = \frac{\mu_0 d}{w} \tag{3.19},$$

where, d is the height of MLGNR over a ground plane and $\mu_0$is the permeability of free space.

Based on the aforementioned discussion regarding the modeling of circuit parameters, novel equivalent circuit parameters per unit length for the ESC model of MLGNR are given by,

$$R_{ESC} = R_{SC-MLGNR} = \frac{12.9}{n.N_{ch}}\left(1 + \frac{l}{\lambda_{eff}(T)}\right) \tag{3.20},$$

$$L_{ESC} = \mathit{f}(L_K and\ L_m) \tag{3.21},$$

$$C_{ESC} = \mathit{f}(C_q and\ C_e) \tag{3.22}$$

3.3 RLC modeling of copper based interconnects

Additionally, to evaluate the performance of copper interconnects precisely under temperature variations, the following temperature-dependent low bias resistance formula can be used [31].

$$R(T) = R_0[1 + \alpha(T - T_0)] \tag{3.23},$$

here, $\alpha = 0.0039K^{-1}$is the temperature coefficient of resistance measured at room temperature [32]. R_0 is the resistance at room temperature, defined as $R_0 = \frac{\rho_0 l}{A}$. Here, ρ_0 is the resistivity of copper at room temperature [33].

It can be seen from Eqs. (3.14, 3.23), the effective low bias resistance of the MLGNR and Cu is function of temperature.

In order to calculate the other temperature-independent circuit parameters of Cu, the following analytical expressions are used [34-36].

Self-inductance (L_s):

$$L_s = \frac{\mu_0 l}{2\pi}\left[ln\frac{2l}{w+t} + 0.5 + \frac{0.22(w+t)}{l}\right] \quad (3.24)$$

Ground capacitance (C_g):

$$C_g = \epsilon\begin{bmatrix}\frac{w}{d} + 2.22\left(\frac{s}{s+0.7d}\right)^{3.19} \\ +1.17\left(\frac{s}{s+1.15d}\right)^{0.76}\left(\frac{s}{t+4.53d}\right)^{0.12}\end{bmatrix} \quad (3.25)$$

Coupling Capacitance (C_c): This is the capacitance between adjacent interconnects [31].

$$C_c = \epsilon\begin{bmatrix}1.14\frac{t}{s}\left(\frac{d}{d+2.06s}\right)^{0.09} + 0.74\left(\frac{w}{w+1.59s}\right)^{1.14} \\ +1.16\left(\frac{w}{w+1.87s}\right)^{0.16}\left(\frac{d}{d+0.98s}\right)^{1.18}\end{bmatrix} \quad (3.26),$$

here, *l* represents length of interconnects, *w* is the width, *d* is the height above ground, *t* is the thickness, *s* is the separation between adjacent interconnects, ε is the dielectric constant and μ_0 is permeability.

3.4 Conclusion

Thermally aware circuit modeling is presented in this chapter by considering an equivalent single conductor (ESC) model of MLGNR. Based on types of contact two different resistance models of MLGNR, top contact MLGNR and side contact are explained. It is seen that SC-MLGNR has less resistance than TC-MLGNR and for further analysis SC-MLGNR model is considered. Effect of different types of scattering is also considered while modeling the mean free path (MFP). RLC parameters of copper based interconnects are also presented.

CHAPTER 4

THERMALLY AWARE IMPEDANCE ANALYSIS OF MLGNR INTERCONNECTS

4.1 Introduction

Number of connections between the devices has increased with the downscaling of technology, leading to a higher wiring density and therefore the reduction in interconnect dimensions. Thus, reduction in dimensions of interconnects resulted in higher resistivity of copper. Values of R, L and C highly influence the performance of interconnects. Because of better RLC parameters than copper, many researchers have proposed MLGNR as future VLSI interconnects.

In this chapter, thermally aware impedance analysis for both MLGNR and copper based interconnects is presented at 22nm technology node. Resistance, inductance and capacitance values are calculated for different global lengths of interconnect ranging from 200μm to 1000μm. Variations in resistance of MLGNR and copper with temperature ranging from 300K to 500K are analysed. It is seen that temperature has significant role in resistance values of MLGNR and copper based interconnects. Impedance parameters of MLGNR are found to have lesser values than copper based interconnects. Temperature independent resistance model of MLGNR based interconnects is also analysed.

4.2 Impedance analysis of MLGNR and copper interconnects

In this section, thermally aware impedance analysis for both MLGNR and copper based interconnects are presented at *22nm* technology node. Physical parameters for interconnects are taken from the latest ITRS-2012 [1] as illustrated in Table 4.1. In this present study, effect of edge roughness is not considered. X. Chuan *et al.* [6] has reported that edge roughness degrades the performance of GNR. Circuit models presented in chapter 3 are used for the impedance analysis of MLGNR and copper interconnects.

Table 4.1: Simulation Parameters-ITRS 2012 [1].

Technology Node 22nm	**Local**	**Semi-Global**	**Global**
Width of Global interconnect (*w*)	19nm	19nm	29nm
Separation between adjacent interconnect nets (*s*)	19nm	19nm	29nm
Thickness of interconnect(*t*)	38nm	38nm	68nm
Oxide thickness(*d*)	38nm	35nm	44nm
ϵ_r	4.2	3.25	3.25
ρ_{Cu}**(μΩ.cm)**	6.96	6.96	5.26

Mean free path (MFP) of electron of MLGNR is a function of temperature as can be seen from the Eq. (3.7). In Fig. 4.1 mean free path is plotted against temperature over a range from 300K to 500K. It can be seen that MFP is inversely proportional to temperature, as its value decreases with the increase in temperature. This is due to the fact that scattering increases as temperature rises above the room temperature.

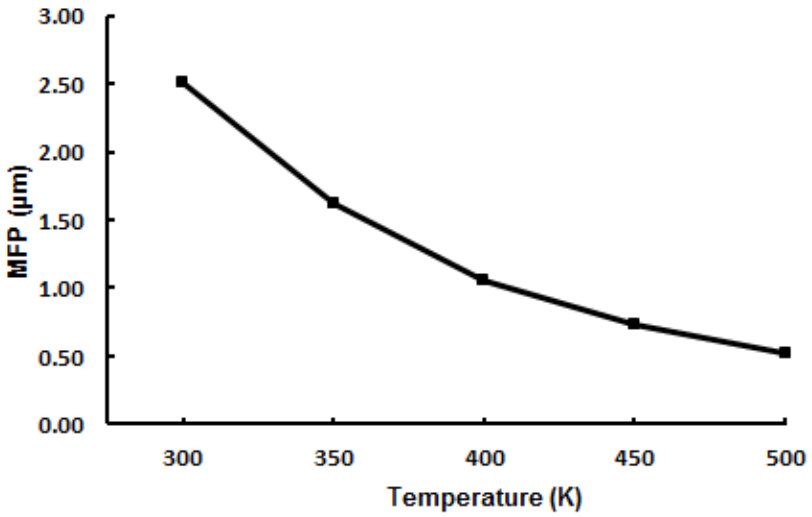

Fig. 4.1. Mean free path as a function of temperature.

It can be seen from Eqs. (3.14, 3.23) that the low bias resistance of both MLGNR and Cu is a function of thermally aware MFP of electrons. In Figs. 4.2 and 4.3, the variation of low bias resistance at different lengths of interconnect with rise in temperature, ranging from *300K* to *500K*, are exhibited for MLGNR and copper, respectively.

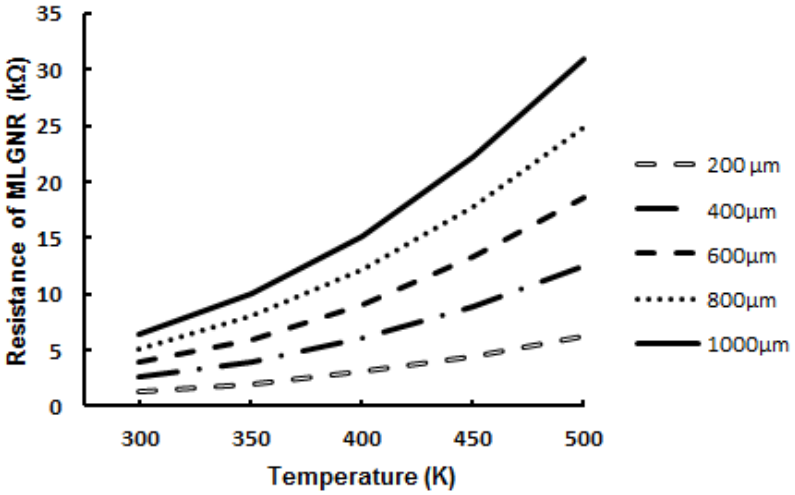

Fig. 4.2. Resistance of MLGNR interconnects as a function of temperature for different lengths.

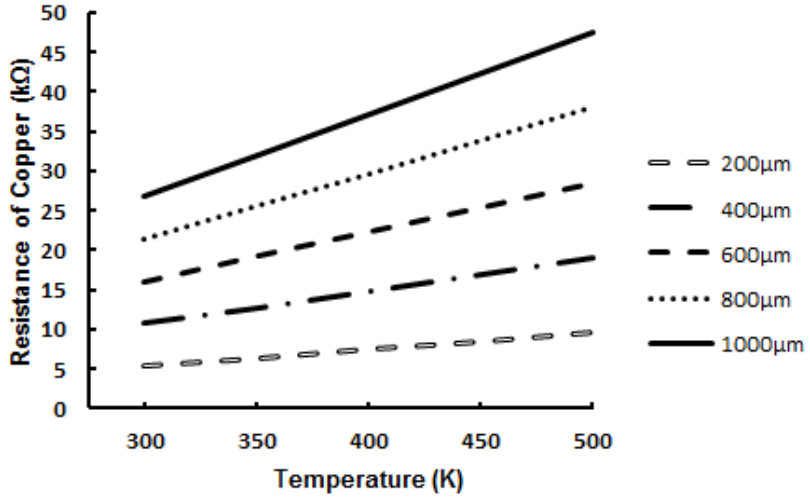

Fig. 4.3. Resistance of Cu interconnects as a function of temperature for different lengths.

It is found that the resistance increases with rise in temperature at different lengths of interconnect for both MLGNR and copper. However, the resistance of copper interconnects, at any specific temperature, in the range *300K* to *500K*, is many times larger than that of MLGNR at different lengths. This is because of weak variation of temperature dependent scattering on the mean free path of MLGNR electrons as compared with that of copper counterpart. It has also been noted from Figs. 4.2 and 4.3 that, compared to smaller interconnects, longer interconnects are more affected by temperature.

From Fig. 4.4 it may be noted that for 1mm long interconnect MLGNR is having smaller resistance values than copper interconnects. Thus, in the context of reducing

voltage noise level and time duration of output transient response, compared with Cu interconnects, MLGNR interconnects are more favourable.

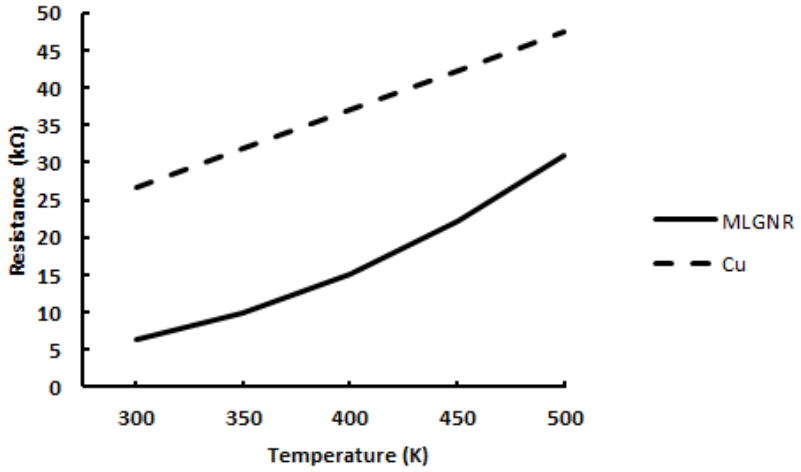

Fig. 4.4. Resistance of MLGNR and copper based interconnects at different temperatures for 1mm long interconnects.

Further, temperature independent model of MLGNR resistance is considered and value of MFP is taken as 1μm as suggested in [6-7, 19]. In Fig. 4.5 resistance values obtained from temperature dependent and temperature independent model of MLGNR resistance are plotted w.r.t. length of interconnects ranging from 200μm to 1000μm. It can be seen that thermally aware model has lesser resistance values than temperature independent model of MLGNR. Thus, it can be said that thermally aware performance analysis of MLGNR is important to consider its possibility as a future VLSI interconnects material.

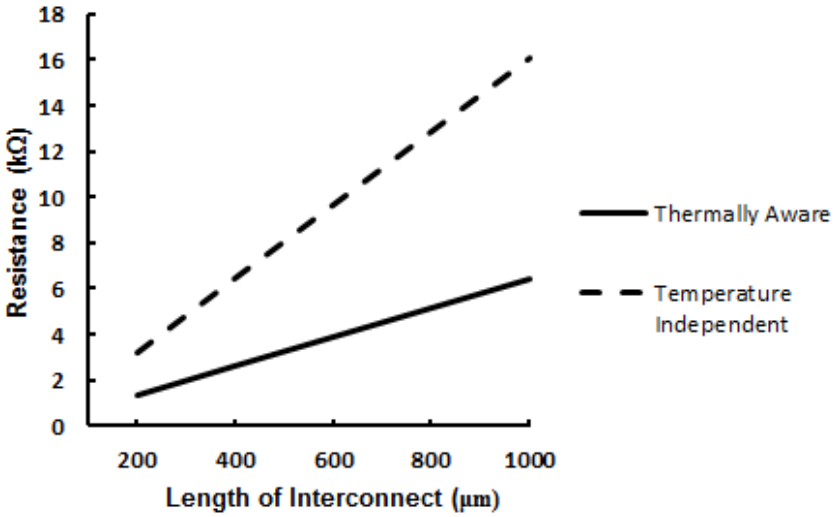

Fig. 4.5. Resistance of thermally aware and temperature independent model of MLGNR at different lengths of interconnects.

Other equivalent circuit parameters viz. capacitance and inductance are calculated for both MLGNR and copper using Eqs. (3.15)-(3.19) and (3.24)-(3.25) respectively. These

values are plotted against different lengths of interconnects in Fig. 4.6 and 4.7. It can be seen that with increase in length of interconnects both capacitance and inductance increases for both the interconnects.

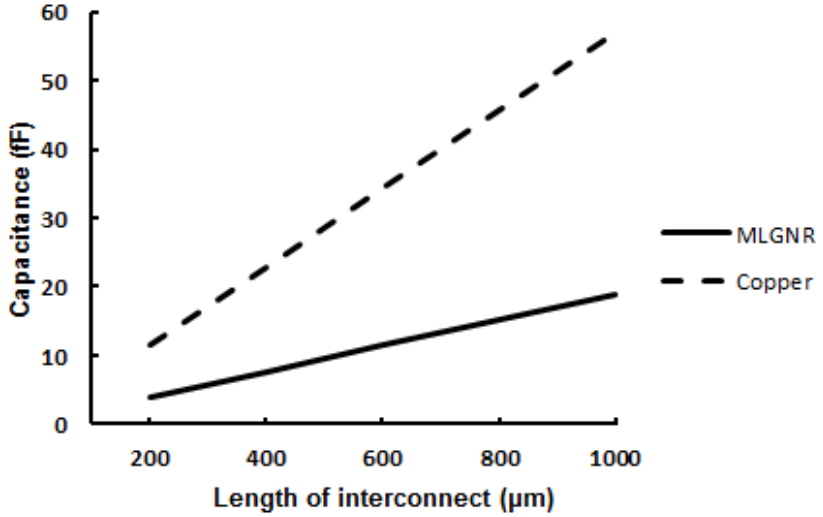

Fig. 4.6. Capacitance of MLGNR and copper interconnects w.r.t. length of interconnects.

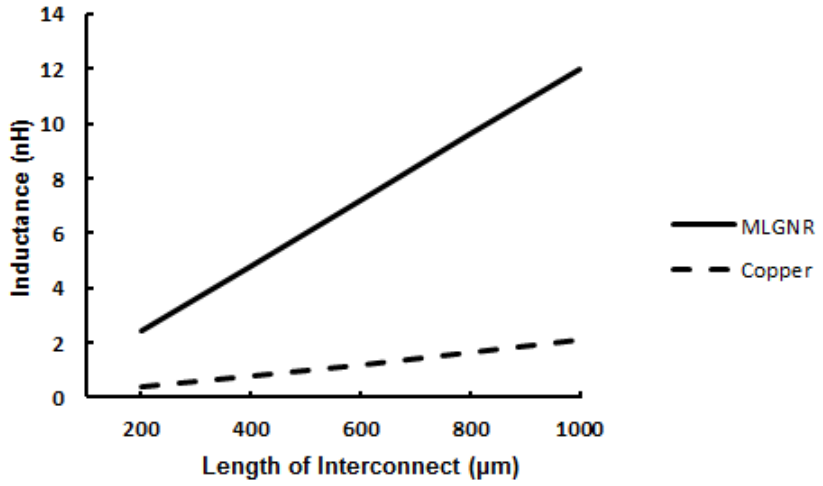

Fig. 4.7. Inductance of MLGNR and copper interconnects w.r.t. length of interconnects.

Most investigators of carbon material based interconnects take the value of coupling capacitance as equivalent to that of the coupling effect between metal interconnects of the same dimensions [36-37, 41]. Based on this theory, coupling capacitance of MLGNR interconnect is assumed to be equal to that of copper interconnects with same dimensions. Hence, the value of coupling capacitance between adjacent interconnects of MLGNR and Cu is computed by Eq. (3.26) and tabulated in Table 4.2 at *22nm* technology node.

Table 4.2: Impedance parameters of *1mm* global interconnect: Temperature=*300K*, Technology-*22nm.*

Length of Interconnect (µm)	**MLGNR**			
	Resistance (Ω)		**Inductance (nH)**	**Capacitance (fF)**
	Temperature Dependent	**Temperature Independent**		
200	1298	3235	2.39	3.79
400	2581	6454	4.79	7.59
600	3863	9673	7.18	11.4
800	5146	12893	9.57	15.2
1000	6428	16112	12.0	19.0

Length of Interconnect (µm)	**Copper**		
	Resistance (Ω)	**Inductance (nH)**	**Capacitance (fF)**
200	5335	0.35	11.4
400	10669	0.76	22.8
600	16004	1.19	34.3
800	21339	1.63	45.7
1000	26673	2.09	57.1

4.3 Conclusion

Mean free path (MFP) of MLGNR is found to be very sensitive to temperature. Resistance of MLGNR depends upon mean free path and thus, changes rapidly with temperature. It is found that the resistance of both copper and MLGNR interconnects increases with increase in temperature. Resistance of copper increases linearly with temperature and resistance of MLGNR show nonlinear increase with temperature. Impedance analysis shows that the MLGNR has lower resistance; capacitance and inductance values than copper interconnects at different range of interconnect lengths. Comparing the temperature dependent resistance model with temperature independent resistance model of MLGNR it is clearly seen that a thermally aware performance analysis of MLGNR is must for accurate modeling.

CHAPTER 5

THERMALLY AWARE PERFORMANCE ANALYSIS OF MLGNR INTERCONNECTS

5.1 Introduction

Temperatures variations above room temperature have a significant effect on interconnect performance in terms of delay and crosstalk. This is because the resistance of interconnects increases with rise in temperature. Therefore, there is an important need to analyse temperature dependent performance of MLGNR as nano-scaled interconnects.

In this chapter, a detailed temperature dependent performance analysis in terms of propagation delay, power dissipation and crosstalk-induced voltage noise of MLGNR based interconnects is presented. Results of thermally aware model are compared with that of conventional temperature independent model of resistance of MLGNR interconnects. Analysis is done for different lengths of interconnect ranging from 200μm to 1000μm with variance in temperature from 300K to 500K. It is found that thermally aware model gives better results than the temperature independent model. As discussed in chapter 2 that many few researchers have studied the impact of crosstalk in MLGNR [10, 21, and 43]. However, no study has been made to analyse the thermally aware crosstalk and delay of MLGNR interconnects so far. First time in this thesis, thermally aware crosstalk-induced voltage noise and delay of MLGNR interconnects at different lengths is presented over a temperature range from 300K to 500K.

5.2 Temperature dependent and independent performance analysis of MLGNR

It is evident from aforementioned discussion in chapters 2 and 3 that the temperature dependent mean free path controls the resistance of MLGNR. Thus, it is important to investigate the temperature dependent performance of MLGNR interconnects. This section includes the performance analysis in terms of power dissipation, propagation delay, and crosstalk of conventionally thermally aware model and temperature-independent model of MLGNR interconnects resistance.

5.2.1 Delay and power analysis

To analyse propagation delay and power dissipation for MLGNR, a distributed RLC circuit of an equivalent interconnect has been considered, shown in Fig. 5.1. Optimum number of repeaters is used for this analysis. The distributed segment is driven by a CMOS driver at *22nm* technology node with V_{dd} = *0.9 V*, a clock speed of 0.1 GHz, and terminated with load capacitive of *0.1fF* [5, 31, and 34]. Driver size is taken equal to 100 for this analysis [6]. This circuit was simulated using Tanner EDA Tools, schematic of a CMOS inverter driving VLSI based interconnect is shown in Fig. 5.2

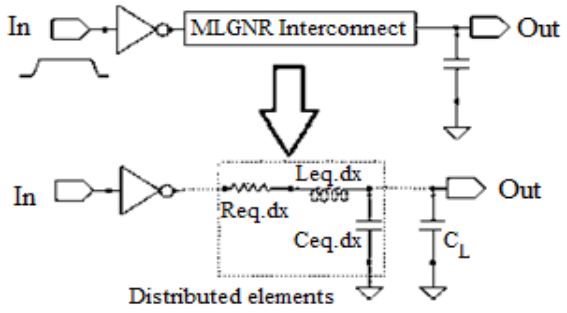

Fig. 5.1. CMOS inverter driven distributed interconnect with load [5].

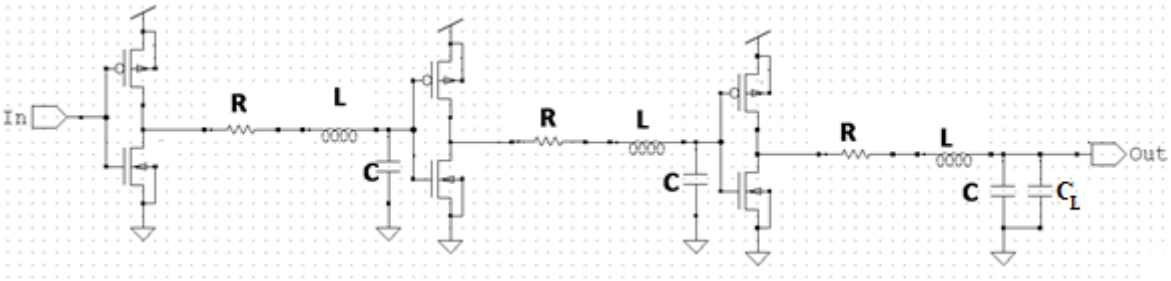

Fig. 5.2. Schematic of a CMOS inverter driving a global interconnect in S-Edit of Tanner EDA.

Pulse waveform with rise time and fall time of 1ns is given at the input port. Data used for simulation is tabulated in Table 4.1.

5.2.1.1 Delay analysis

For delay analysis of MLGNR, 90% propagation delay is calculated w.r.t. temperature at different lengths of interconnects ranging from 200µm to 1000µm and the same is plotted in Fig. 5.3. From this figure it is noted that the propagation delay of MLGNR is increasing with increase in temperature. It can be seen that the variations in delay with temperature are lesser for smaller lengths than for longer lengths of MLGNR based

interconnects, this is because of smaller impedance values at smaller lengths of interconnects as discussed in chapter 4.

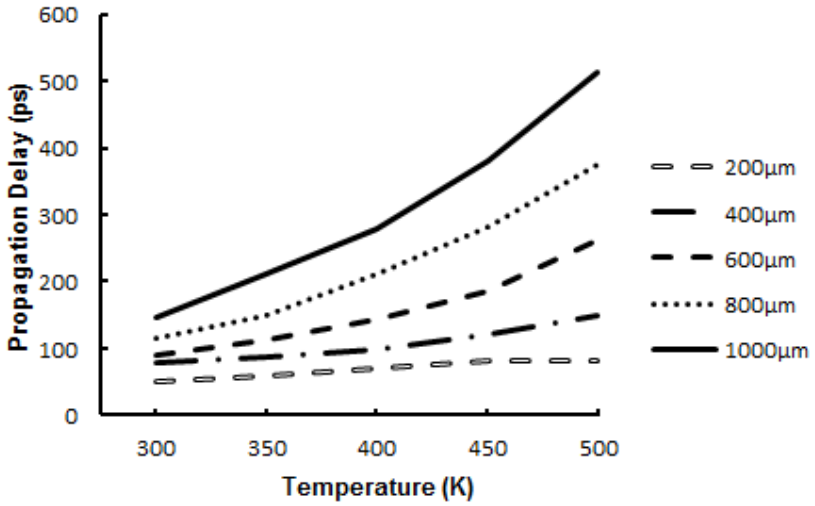

Fig. 5.3. Propagation delay of MLGNR w.r.t. temperature.

Further, in Fig. 5.4 propagation delay of MLGNR of thermally aware model is compared with conventional temperature independent model of resistance. It is found that temperature independent model gives higher delay than temperature dependent model. This is because of lower mean free path of electrons and hence, the higher resistance values in temperature independent model in comparison with thermally aware model of MLGNR resistance.

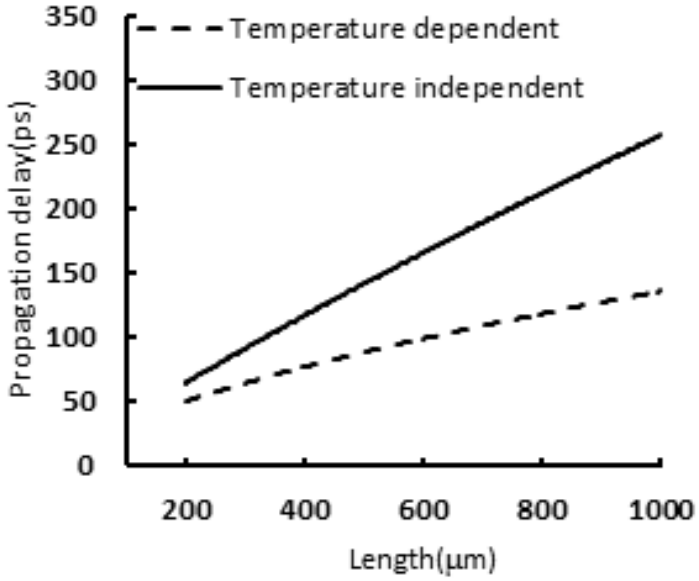

Fig. 5.4. Propagation delay of MLGNR for temperature dependent and independent resistance models at different lengths.

Moreover, average relative improvement in propagation delay using temperature-dependent model instead of temperature independent is shown in Table 5.1. An average relative improvement of 37.24% is achieved in temperature dependent model in comparison with conventionally used temperature independent model of MLGNR resistance.

Table 5.1: Average relative improvement in delay.

S.No.	Length of Interconnect (*μm*)	Delay improvement (%)
1	200	30.14
2	400	21.39
3	600	37.15
4	800	46.92
5	1000	50.6
Average improvement		37.24

5.2.1.2 Power dissipation analysis

As the use of portable communication equipment is growing, the effect of power induced by interconnects become a main concern of VLSI industry. Variations in power dissipation of MLGNR based interconnects w.r.t. different lengths of interconnect is shown in Fig. 5.5. This figure reveals that the power dissipation does not change much with change in temperature above room temperature for a particular length of interconnects. This is because of constant capacitance value at specific interconnect length of MLGNR.

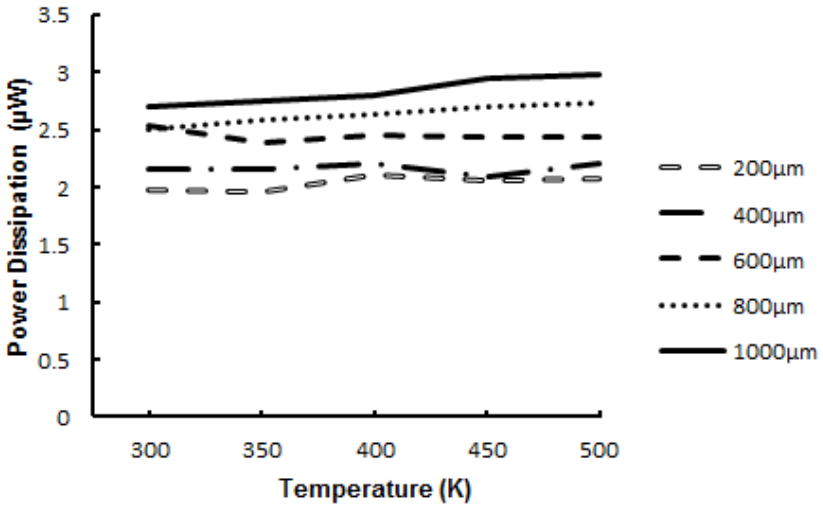

Fig. 5.5. Power dissipation of MLGNR w.r.t. temperature

Further, Fig. 5.6 shows the comparison between results obtained in terms of power dissipation through temperature-dependent and independent model of MLGNR

resistance as a function of interconnect length. In this comparison, a temperature dependent model of resistance is considered at *300K*.

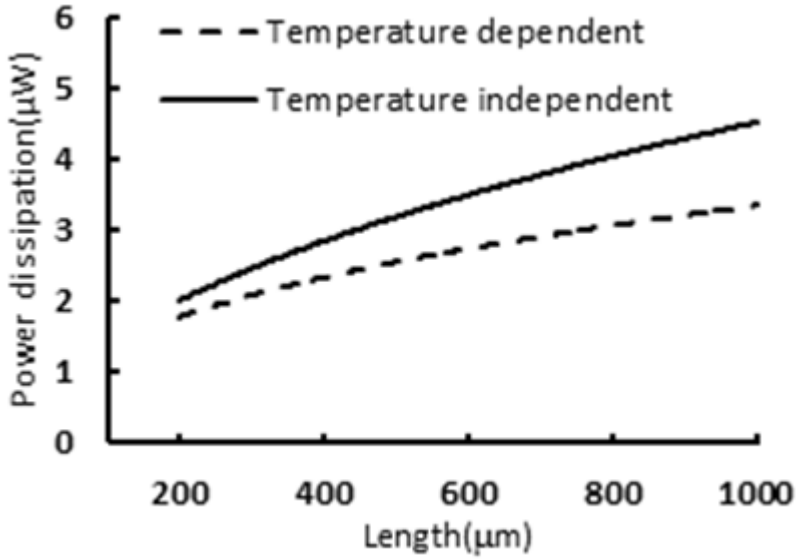

Fig. 5.6. Power Dissipation of MLGNR for temperature dependent and independent resistance models at different lengths.

It is seen from Fig. 5.6 that the variations of power dissipation, calculated using temperature dependent model of MLGNR resistance for varied lengths, is always lesser than that of the conventional temperature independent model of resistance. This is because of the impact of lower value of temperature dependent resistance compared to temperature independent resistance at any specific length in the range *200μm* to *1000μm* (Table 4.2). Further, it may also be noted that power dissipation, under two different cases of resistance, increases with length. This is because, with increased length, circuit parameters (R, L and C) increase, and so the power dissipation also increases.

From Table 5.2 it can be seen that compared to a temperature independent model of MLGNR resistance the average relative improvement in power dissipation is achieved about 26.34%, respectively, using temperature-dependent model for the all interconnect lengths.

Table 5.2: Average relative improvement in power dissipation.

S.No.	Length of Interconnect(μm)	Power dissipation Improvement (%)
1	200	4.37
2	400	26.03
3	600	19.68
4	800	36.51
5	1000	45.12
Average improvement		26.34

5.2.2 Crosstalk analysis

As the integration density of interconnects increases with aggressive technology scaling, crosstalk effects will become increasingly valuable in a VLSI chip [31, 38, 40-42]. Hosseini *et al.* [18] stated that high performance integrated circuits have a great variance in temperature. These temperature variations have a significant effects on the crosstalk induced noise voltage between coupled interconnects. However, no account of temperature dependent crosstalk induced voltage noise in coupled MLGNR interconnects has been reported. Hence, there is a need to study the thermally aware crosstalk-induced voltage noise in scaled deep sub-micron (DSM) CMOS technologies for MLGNR interconnects.

In this section, the temperature dependent crosstalk induced voltage noise waveform at the far end of victim line in capacitively coupled MLGNR interconnects has been analysed for the first time, at *22nm* technology node. Further, a detailed investigation of time duration of the victim output waveforms between temperature-dependent and conventional (temperature-independent model) model of MLGNR interconnects resistance is presented at different lengths.

To examine the crosstalk voltage noise, a capacitively coupled RLC distributed interconnects circuit (as shown in Fig. 5.7) has been considered. All the signal wires are driven by a CMOS driver at *22nm* technology node [35] with a clock speed of *0.1 GHz*, V_{dd} *= 0.9V*, fall time = *1ns*, rise time = *1ns* and terminated with capacitive load of *0.1fF* [29, 31]. For crosstalk analysis, the crosstalk affected net (victim net) is kept fixed at logic *1* and the net that cause crosstalk on victim (aggressor net) are switched from logic *1→0*. For all calculation and simulation purposes, the data shown in Table 4.1 have been used.

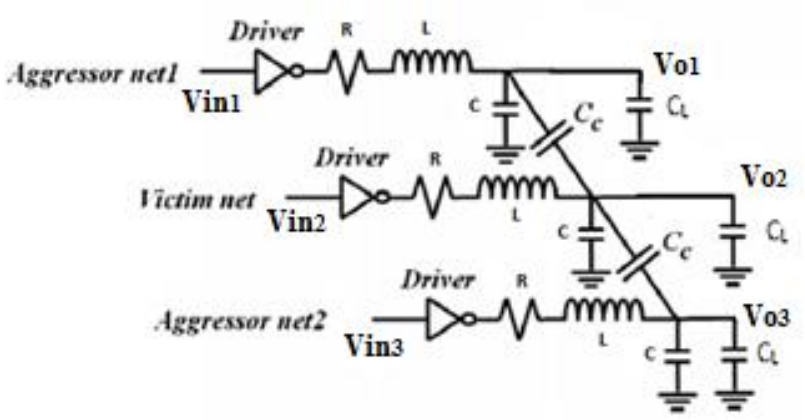

Fig. 5.7. Capacitively coupled distributed circuit to model crosstalk between adjacent nets [36].

Fig. 5.8 illustrates the crosstalk-induced transient response of the victim output for varied temperatures for MLGNR based interconnects and deliver an insight into the temperature variation of interconnect resistance (see Fig. 4.2). It is observed that the transient variation of crosstalk-induced noise voltage level decreases for MLGNR interconnect with rise in temperature from *300K* to *500K*.

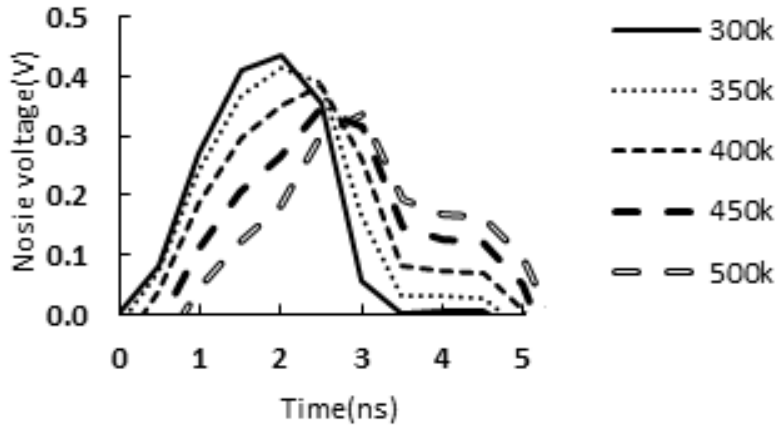

Fig. 5.8. Thermally aware Crosstalk induced transient response of capacitively coupled interconnects for MLGNR at victim far end.

Fig. 5.9 explains the dependence of normalized time duration on the interconnect length *(l)* at *22nm* technology node under two different cases temperature-dependent and independent model of a MLGNR resistance. Temperature-dependent model of MLGNR resistance is considered at *300K*. For a temperature independent model of resistance,

MLGNR interconnects with a mean free path of *1μm* has been considered [6]. The time duration values have been normalized by their respective values obtained at *300K*.

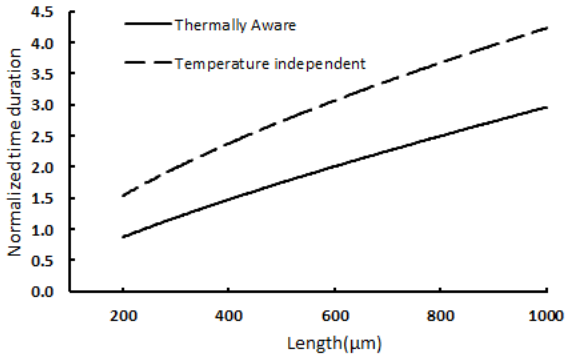

Fig. 5.9. Normalized time duration as a function of interconnect length of victim output.

It is seen that, in both cases (temperature independent and thermally aware model of resistance), the normalized time duration of the victim output waveform increases monotonically with an increase in interconnect length. The changes are basically reflections of the interconnect length *(l)* variations on the resistance of MLGNR interconnects. It may also be observed from Fig. 5.9 that the normalized time duration obtained using a temperature independent model is more compared to thermally aware model of MLGNR resistance for the whole range of interconnect length. This is because of lower values of thermally aware resistance of MLGNR for different lengths (see Table 4.2).

In addition, it can be seen from Table 5.3 that, there is an average relative improvement of about 35% in the time duration reduction of transient responses at the far end of victim output by using temperature dependent model instead of conventional temperature independent model of MLGNR resistance for the whole range of interconnect lengths.

Table 5.3: Average improvement in accuracy of coupled victim output pulse width estimation using thermally aware model in comparison of temperature dependent model.

Length of interconnect (*μm*)	**Improved reduction in time duration of transient response at the output of victim (%).**
200	43.32
400	29.25
600	46.84
800	36.36
1000	19.41
Average	35.04

5.3 Conclusion

Delay and power analysis of MLGNR with variations in temperature from 300K to 500K is shown in this chapter. SPICE simulation reveals that for frequency of 0.1 GHz, MLGNR interconnects give propagation delay in range of 50ps to 500ps at different lengths of interconnect ranging from 200μm to 1000μm as the temperature varies from 300K to 500K. Power dissipation due to MLGNR interconnects is found to be ranging from 2μW to 3μW. Moreover, an average improvement of 37.24% and 26.34% in propagation delay and power dissipation respectively is observed using thermally aware model of resistance instead of temperature independent model of resistance of MLGNR interconnects at different interconnect lengths ranging from 200μm to 1000μm. While doing crosstalk analysis, an average relative improvement in the time duration reduction of victim output, for the same range of interconnect lengths, is achieved about 35% by using a temperature-dependent model instead of a temperature independent model of MLGNR resistance.

CHAPTER 6

A COMPARATIVE ANALYSIS BETWEEN MLGNR AND COPPER INTERCONNECTS

6.1 Introduction

As the feature size is decreasing, problems of electro-migration, surface scattering and grain boundary scattering in copper interconnects are getting worse. Hence, there is a need to find alternative material to be used as VLSI interconnects. In recent years, researchers have suggested MLGNR as a promising interconnect material. But, MLGNR is yet to be compared with copper with the variance in temperature.

In this chapter, performance analysis of copper based interconnects is done and then performance of MLGNR based interconnects is compared with conventionally used copper interconnects on the basis of propagation delay, power dissipation and crosstalk voltage noise. This comparison is done at different lengths of interconnect ranging from 200μm to 1000μm over a temperature range of 300K to 500K. It is found that the MLGNR gives far better results than the copper based interconnects.

6.2 Performance analysis of copper based interconnects

Similar simulations have been carried out for Cu based interconnects at same technology and clock speed as are described for MLGNR in the previous chapter. Same circuit shown in Fig.5.2 is used for delay and power analysis of copper interconnects.

6.2.1 Delay analysis of copper

After doing the delay analysis results obtained are shown in Fig. 6.1. It can be seen that propagation delay increases with increase in temperature for all interconnect lengths. Increase in delay is less for smaller lengths in comparison to longer lengths of interconnects because the change in resistance values is less for smaller lengths (see Fig. 4.3).

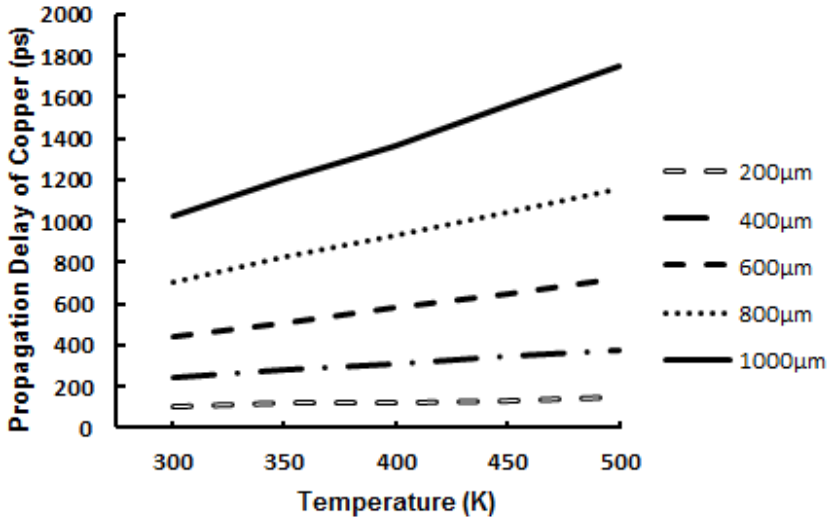

Fig. 6.1. Propagation delay of copper interconnects w.r.t. temperature at different lengths.

6.2.2 Power analysis of copper

Power analysis of copper is done in same way as described for MLGNR interconnects in chapter 5. Power dissipation values obtained from SPICE simulation are plotted in Fig. 6.2. It can be seen that power dissipation increases with increase in interconnect length. Figure also reveals that power dissipation of copper based interconnects is almost constant over entire temperature range. This is because of constant capacitance and inductance values at specified lengths with variation in temperature (chapter 4).

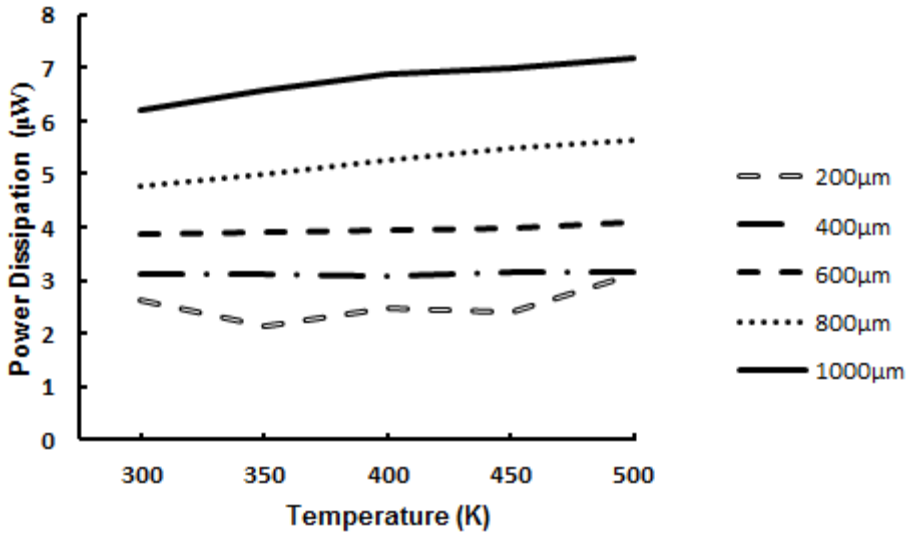

Fig. 6.2. Power dissipation of copper interconnects w.r.t. temperature at different lengths.

6.2.3 Crosstalk analysis of copper

To examine the crosstalk voltage noise of copper based interconnects, a capacitive coupled RLC distributed interconnects circuit has been considered as shown in Fig. 5.7. All the signal wires are driven by a CMOS driver at *22nm* technology node [34] with same clock speed and pulse as for the case of MLGNR (section 5.2.2).

Thermally aware crosstalk induced transient response of capacitively coupled interconnects for Cu at victim far end is shown in Fig. 6.3. It may be noted that the peak voltage noise is decreasing with the increase in temperature. This is because the resistance of Cu based interconnects increases with increase in temperature, so the voltage drop across inductance parameters increases and hence, the voltage value at victim output decreases.

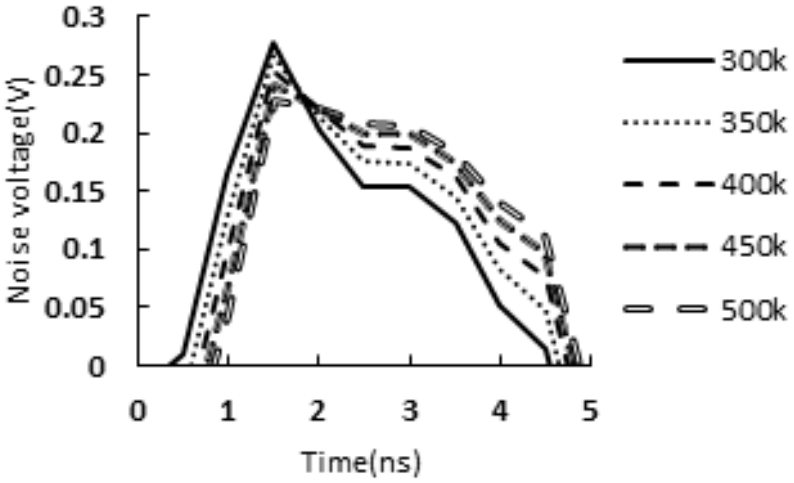

Fig. 6.3. Thermally aware crosstalk induced transient response of capacitively coupled interconnects for copper at victim far end.

6.3 Results and comparative analysis

As the temperature increases above the room temperature performance of VLSI interconnect degrades [18]. Many researchers have proposed carbon-nanotube based interconnects as an alternative to copper interconnects because of negative effects of temperature on its performance [44-46]. Balandin *et al.* [47] have measured the thermal conductivity of single layer graphene and found it superior to that of carbon nanotube. Due to its remarkable properties multilayer graphene nano-ribbon (MLGNR) is

considered as an important interconnect material. Hence, it is important to compare conventionally used copper based interconnects with MLGNR based interconnects.

In this analysis, results obtained from performance analysis of MLGNR (chapter 5) and copper (section 6.2) are analysed and compared.

6.3.1 Comparative delay and power analysis

Propagation delay and power dissipation of copper interconnects are used to normalize corresponding MLGNR-interconnect propagation delays and power dissipations, respectively. Fig. 6.4 illustrates the dependence of *90%* propagation delay ratio (MLGNR/Cu) on temperature, ranging from *300K* to *500K*, for long (*1mm*) interconnect. It is observed that the normalized delay increases with rise in temperature, but this variation is observed more in Cu based interconnects. The variation is simply a reflection of the effect of temperature variation on resistance for both MLGNR and copper (see Figs. 4.2 and 4.3).

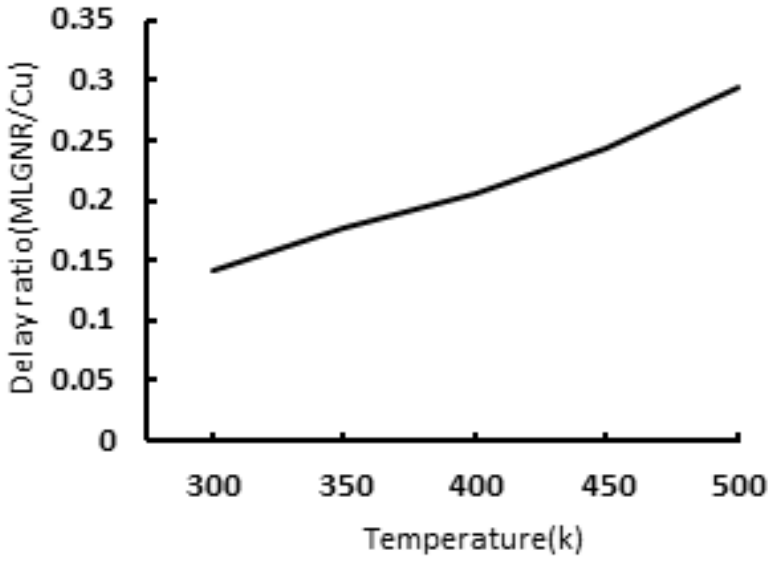

Fig. 6.4. Delay ratio with varying temperature for long interconnect (*1mm*) at 22nm technology node.

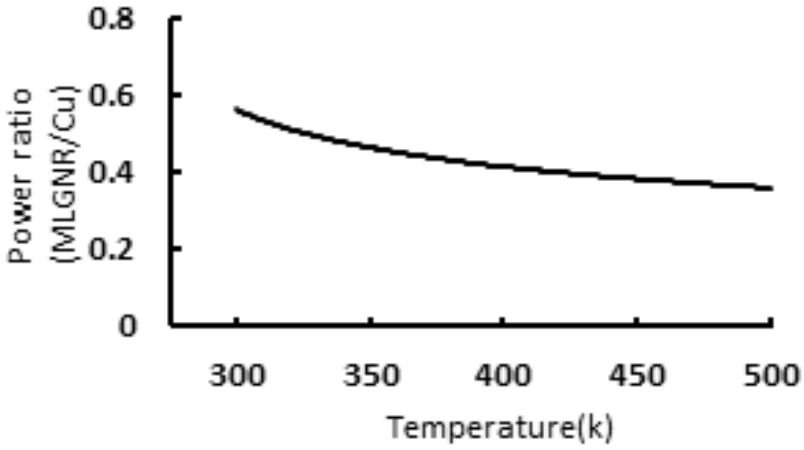

Fig. 6.5. Power ratio with varying temperature for 1mm long interconnects at 22nm technology node.

Nowadays, overall power is dramatically increasing with scaling of technology in deep sub-micron. Therefore, the effect of power dissipation induced by interconnects in advance technology nodes become a prime concern for VLSI industry [5, 39, and 48]. A power dissipation ratio (MLGNR/Cu) for long (*1mm*) interconnect with increase in temperature, ranging from *300K* to *500K*, is illustrated in Fig. 6.5 at *22nm* technology node. It is found that the ratio of power dissipation of MLGNR to copper, at any specific temperature, in the range *300K* to *500K*, is less than unity. That means copper dissipate more power than MLGNR with rise in temperature due to higher value of interconnect capacitance (see Table 4.2). It may also be noted that the power ratio decreases with rise in temperature and remains almost constant for a higher temperature (*≥450K*). This is because of the relative percentage change in MLGNR resistances at higher temperature is less in MLGNR, compared to copper, depicted in Fig. 6.6. The relative percentage change in MLGNR resistances w.r.t. copper in Fig. 6.6 is extracted from Fig. 4.2 and 4.3 for *1mm* long interconnects.

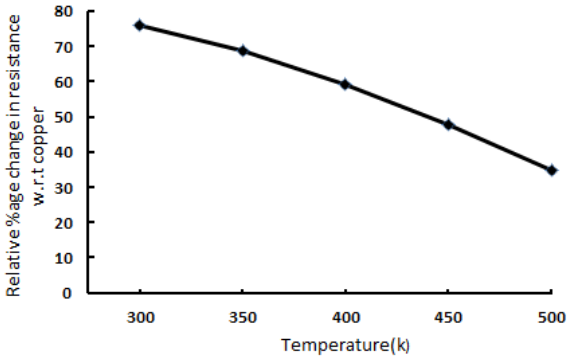

Fig. 6.6. Relative percentage change in resistance w.r.t. copper for 1mm long interconnect.

6.3.2 Comparative crosstalk analysis

The impact of temperature variation on normalized crosstalk-induced noise voltage level (positive peak voltage) of victim output is shown in Fig. 6.7 for both MLGNR and Cu. The normalized crosstalk-induced positive noise voltage peak at the far end of victim line, defined as the ratio between the terminal voltage victim output and the input voltage of the aggressor (V_{o2}/V_{in}). The result reveals that the crosstalk-induced positive noise voltage peak reduces with rise in the temperature. This is because of the fact that as resistance increases; the voltage steps arriving at the far end of the line are smaller and have larger time duration [31, 38, and 40].

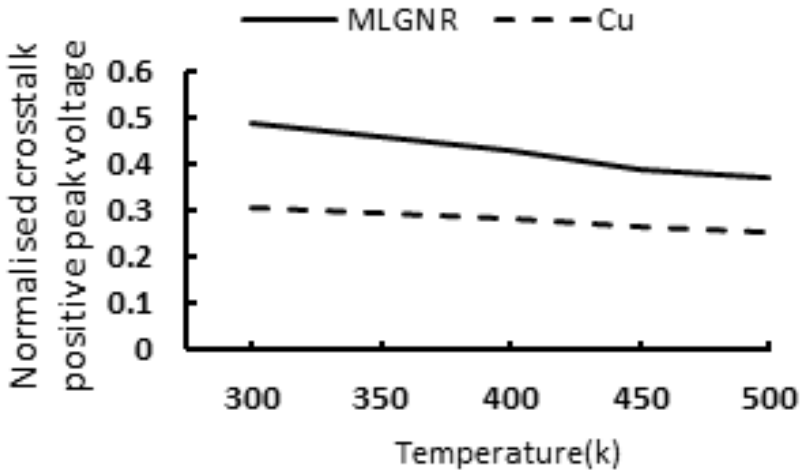

Fig. 6.7. Variation of normalized crosstalk induced positive noise voltage peak with temperature at the far end of the victim line.

The result also illustrates that coupled copper interconnects have comparatively lower crosstalk-induced positive noise voltage peaks, because of the control of its smaller self-inductance (L_s) and a larger ground capacitance (C_g) compared with MLGNR. It is reported [40], as self-inductance of interconnect is increased and ground capacitance decreased, then even and odd mode characteristic impedances increase, triggering positive peak voltage to increase significantly.

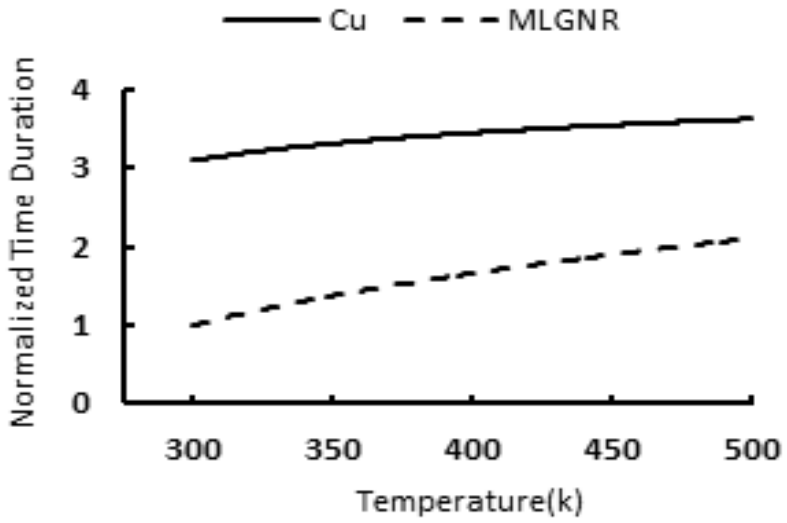

Fig. 6.8. Normalized time duration of the victim output waveform for both MLGNR and copper.

Fig. 6.8 shows that the normalized time duration of the victim output waveform of both MLGNR and Cu interconnects depends on temperature. The values of time duration have been normalized by their respective values obtained at *300K* for both MLGNR and copper. It is observed that the time duration of both coupled interconnects of MLGNR and copper, monotonically increasing with rise in temperature. This is due to increase in resistance values with increased temperature and thus the time duration also increases as discussed in the previous paragraph. In addition, it has also been noted that the time duration of MLGNR is always lower than the copper interconnects as the temperature is varied from *300K* to *500K*. This is due to higher resistance values of copper at any specific temperature in the range *300K* to *500K*. It is found that the thermally aware crosstalk induced delay in MLGNR, at the far end of aggressor, is always less than the copper. But compared with its single line MLGNR delay (see Fig. 5.3), as the temperature rises, the crosstalk induced propagation delay is observed more because of coupling effects.

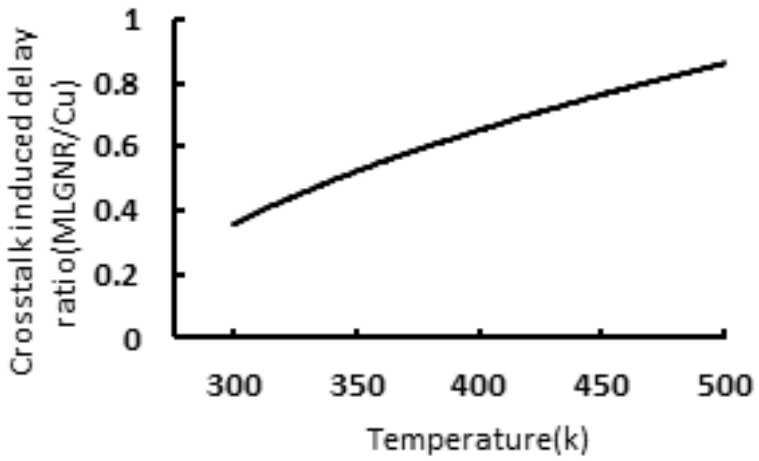

Fig. 6.9. Crosstalk induced delay ratio with varying temperature for 1mm long interconnect at 22nm technology node.

Fig. 6.9 depicts the dependence of the *90%* normalized crosstalk induced delay at the far end of the aggressor on temperature in capacitively coupled interconnects for both MLGNR and copper. Propagation delay of Cu interconnect is used to normalize corresponding MLGNR-interconnect propagation delays at different temperature.

6.3 Conclusion

SPICE simulation shows that the MLGNR based interconnects are much better than copper based interconnects. Due to high resistance values power dissipation and propagation delay of copper based interconnects are found to be higher than MLGNR based interconnects. Crosstalk voltage noise observed at output of victim net of copper is lesser than MLGNR. The time duration of the coupled victim output waveform increases with increase in temperature for both MLGNR and copper interconnects, but the change is observed more in Cu. These results state that MLGNR is far better than copper and can be considered as promising future VLSI interconnects material.

CHAPTER

7 CONCLUDING REMARKS AND FUTURE SCOPE

7.1 Introduction

With the technology scaling, resistivity of Cu is getting large under the combined effects of enhanced surface scattering, grain boundary scattering, and the presence of a highly resistive diffusion barrier layer in deep-submicron technology nodes. Temperature variation above room temperature has a significant effect on interconnect performance in terms of delay and crosstalk. These are the vital parameters that limit the efficiency of Cu in future technology nodes. Thus, as the resistivity of copper is increasing, there is a need to find its replacement.

In this chapter, concluding remarks of different chapters of the thesis are presented in section 7.2. It has been concluded that, with rise in temperature from 300K to 500K, the MLGNR is a strong alternative interconnect material to replace conventional Cu based interconnects. Further in section 7.3, suggestions for future work in field of MLGNR interconnects are stated.

7.2 Summary of important findings

An overview of the exploratory research on graphene nano-ribbon (GNR) as possible VLSI interconnects is presented in **chapter 2**. With the advancement in technology, limitations of copper have been briefly examined. The work carried out by researchers in finding an alternative solution indicates that the carbon based interconnects have the potential to replace Cu in future. Many researchers proposed graphene nano-ribbon (GNR) as one of the promising candidate materials for both interconnects and transistors.

Thermally aware circuit modeling of MLGNR interconnects is presented in **chapter 3**. Additionally, RLC parameters of copper are also given in same chapter that are further used in performance analysis of copper based interconnects. Resistance of side contact MLGNR is found to be lesser than top contact MLGNR.

Temperature dependent impedance analysis for MLGNR with smooth edges and copper has been done in **chapter 4**. It has been found that the resistance of both MLGNR and copper increases with increase in temperature. Impedance parameters are calculated at different global lengths over a temperature range of 300K to 500K for 22nm technology node. Impedance parameters of MLGNR are having lesser values than copper based interconnects. Impedance analysis has shown that thermally aware performance analysis of MLGNR based interconnects is very important.

In **chapter 5**, thermally aware performance analysis of MLGNR has been investigated. SPICE simulation is used to compare temperature dependent model of MLGNR resistance with temperature independent model on the basis of propagation delay, power dissipation and crosstalk induced voltage noise for 22nm technology node. An average relative improvement of 37.24% and 26.34% in propagation delay and power dissipation respectively is achieved by using temperature-dependent model instead of temperature independent model of MLGNR resistance, with length variations from 200μm to 1000μm. Crosstalk analysis results reflect that there is an average relative improvement of about 35% in the time duration reduction of victim output, for the same range of interconnects lengths, by using a temperature-dependent model instead of a temperature independent model of MLGNR resistance.

In **chapter 6**, performance of MLGNR based interconnects was compared with copper based interconnects on the basis of propagation delay, power dissipation and crosstalk induced voltage noise. SPICE simulation results obtained clearly declare MLGNR as the winner. Delay ratio and power ratio of MLGNR w.r.t copper are having a value less than unity which indicates that MLGNR is having less delay and power than copper interconnects at different lengths ranging from 200μm to 1000μm. It is found that for temperature variations above room temperature MLGNR performs better than copper interconnects. The MLGNR based capacitively coupled interconnect nets gave better crosstalk performance than that of copper counterpart.

It is evident from the present study, compared to copper; the resistance of MLGNR interconnects shows weak dependence on temperature. This significantly reduces the delay variations and crosstalk induced time duration of the victim line due to thermal variations, and is an important advantage over copper interconnects.

In brief, the analysis and simulations done till now show that if a GNR technology with smooth edges and compatible with integrated circuit technology can be developed, then it will be likely to change Cu interconnects by MLGNR based VLSI interconnects.

7.3 Suggestions for future work

In this thesis, it is seen that multilayer graphene nano-ribbon (MLGNR) can be used instead of Cu as an interconnect material for the 22nm technology node due to high current density and high mean free path. Some suggestions for future work in the area of MLGNR interconnects are stated below:

- There is a problem of edge roughness that degrades MLGNR's performance. So, there is a lot of work to do to improve fabrication techniques.
- Performance of MLGNR is yet to be compared with mixed carbon nanotube bundle (MCB) interconnects. MCB interconnects are also strong candidate to replace copper interconnects.

REFERENCES

[1] Semiconductor Industry Association, International Technology Roadmap for Semiconductors (ITRS), 2012 update, [Online]. Available: http://www.itrs.net/.

[2] V. Kumar, S. Rakheja, and A. Naeemi, "Review of Multi-Layer Graphene Nanoribbons for on-chip Interconnect Applications," IEEE 978-1-4799-0409-9/13/$31.00, 2013.

[3] M.K. Rai and S. Sarkar, "Carbon Nanotube as a VLSI Interconnect", Electronic Properties of Carbon Nanotubes, 2011.

[4] C. Xu, H. Li, and K. Banerjee, "Graphene nano-ribbon (GNR) interconnects:A genuine contender or a delusive dream?," in IEDM Tech. Dig., pp. 201–204, Dec. 2008.

[5] M.K. Rai, A.K. Chatterjee, S. Sarkar, and B.K. Kaushik, "Performance analysis of multilayer graphene nanoribbon (MLGNR) interconnects," J Comput Electron. 2016, DOI 10.1007/s10825-015-0786-x.

[6] X. Chuan, L. Hong, and K. Banerjee, "Modeling, Analysis, and Design of Graphene Nano-Ribbon Interconnects," IEEE Transactions on Electron Devices, 56:1567-1578., 2009.

[7] X. Chuan, L. Hong, N. Srivastava, and K. Banerjee, "Carbon Nanomaterials for Next-Generation Interconnects and Passives: Physics, Status, and Prospects," IEEE Transactions on Electron Devices, 56(9), pp. 1799 – 1821, 2004.

[8] K. Geim, and K.S. Novoselov, "The rise of graphene," Nat.Mater, 6(3), pp.183-191, 2007.

[9] N. Srivastava, and K. Banerjee, "Interconnect Challenges for nanoscale electronic circuits," TMS J.Mater, 56(10), pp. 30-31, 2004.

[10] W.S. Zhao, and W.Y. Yin, "Comaparative Study on Multilayer Graphene nanoribbon (MLGNR) Interconnects," IEEE Trans. Electromagn. Compat., 56(3), 2014.

[11] T. Ragheb, and Y. Massoud, "On the modeling of resistance in graphene nanoribbon (GNR) of future interconnects applications," in Proc. IEEE/ACM Int. Conf. Comput.-Aided Des., pp. 593–597, 2008.

[12] M.K. Majumder, M. Kumar, B. K. Kaushik, K. N. Reddy, and S. K. Manhas, "Comparison of propagation delay in single and multi-layer graphene nanoribbon interconnects," 5th International Conference on Computers and Devices for Communication (CODEC), 2012.

[13] V. Kumar, S. Rakheja, and A. Naeemi, “Performance and Energy per Bit Modeling of Multilayer Graphene Nanoribbon Conductors,” IEEE Transactions on Electron Devices, 59(10), pp. 2753-2761, 2012.

[14] G. Chiariello, A. Maffucci, and G. Miano, “A temperature-dependent circuit model for carbon-based on-chip global interconnects”, 2012 12th IEEE International Conference on Nanotechnology (IEEENANO), 2012.

[15] Maffucci, and G. Miano, “Number of Conducting Channels for Armchair and Zig-Zag Graphene Nanoribbon Interconnects,” IEEE Transanction on Nanotechnology, 12(5), 2013.

[16] A.K. Nishad, and R. Sharma, “Analytical Time-Domain Models for Performance Optimization of Multilayer GNR Interconnects,” IEEE J. Sel. Top. Quantum Electron, 201, DOI: 10.1109/JSTQE.2013.2272458., 2014.

[17] V.R. Kumar, M.K. Majumder, N.R. Kukkam, and B.K. Kaushik, “Time and Frequency Domain Analysis of MLGNR Interconnects,” IEEE Transactions on Nanotechnology, 14(3), 2015.

[18] Hosseini, and V. Shabro, “Thermally-aware modeling and performance evaluation for single-walled carbon nanotube-based interconnects for future high performance integrated circuits,” Microelectronic Engineering, 87:1955–1962, Dec. 2008.

[19] S. Rakheja, V. Kumar, and A. Naeemi, “Evaluation of the potential performance of Graphene Nanoribbons as On-Chip Interconnects,” Proceeding of the IEEE; 101(7), 2013.

[20] J. P. Cui,W. S. Zhao,W. Y.Yin, and J. Hu, “Signal transmission analysis of multilayer graphene nano-ribbon (MLGNR) interconnects,” IEEE Trans. Electromagn. Compat., vol. 54, no. 1, pp. 126–132, Feb. 2012.

[21] D. Das,and H. Rahaman, “Crosstalk and gate oxide reliability analysis in graphene nanoribbon interconnects,” In: International Symposium on Electronic System Design (ISED), pp. 182–187, 2011.

[22] S.H. Nasiri, and R. Faez, “Compact formulae for number of conduction channels in various types of graphene nanoribbons at various temperatures,” Mod. Phys. Lett. B, 26(1), pp. 1150004-1–115004-5, 2012.

[23] Naeemi and J. D. Meindl, “Compact physics-based circuit models for graphene nanoribbon interconnects,” IEEE Trans. Electron Devices, vol. 56, no. 9, pp. 1822–1833, Sep. 2009.

[24] E.H. Hawang, S. Adam, and S.D. Sharma, “Carrier transport in two dimensional graphene layers,” Phys.Rev.Lett., 98(18), pp.186806-1-186806-4, 2007.

[25] J. Yan, Y. Zhang, P. Kim, and A. Pnczuk, “Electric field effect tunning of electron-phononcoupling in graphene,” Phys.Rev.Ltt., 98(16), pp.166802-1-166802-4, 2007.

[26] D.A. Areshkin, D. Gunlycke, and C.T. White, “Ballistic transport in graphene nanostrips in the presence of disorder:importance of edge effects,” Nano Lett., 7(1), pp. 204-210, 2007.

[27] Y.W. Tan, Y. Zhang, K. Bolotin, Y. Zhao, S. Adam, E.H. Hwang, S.D. Sharma, H.L. Stormer, and P. Kim, “Measurement of scattering rate and minimum conductivity in graphene,” Phys.Rev.Lett. 99(24), pp.246803-1-246803-4, 2007.

[28] M.K. Rai, and S. Sarkar, “Influence of distance between adjacent tubes on SWCNT bundle interconnects delay and power dissipation”, J. Comput. Electron. 12(4), 796–802, 2013.

[29] M.K. Rai, B.K. Kaushik, and S. Sarkar, “Thermally aware performance analysis of single-walled carbon nanotube bundle as VLSI interconnects”, Journal of Computational Electronics, 2016, DOI 10.1007/s10825-016-0793-6.

[30] H. Kempa, and P. Esquinazi, “Field-induced metal-insulator transition in the c-axis resistivity of graphite,” Phys. Rev. B, 65:241101-1–241101-4, 2002.

[31] M.K. Rai, and S. Sarkar, “Temperature dependant crosstalk analysis in coupled single-walled carbon nanotube (SWCNT) bundle interconnects,” International Journal of Circuit Theory and Applications, 2011, DOI: 10.1002/cta.2013.

[32] D. Giancoli, “Electric currents and resistance. In Physics for Scientists and Engineers with Modern Physics,” Phillips J (ed) (4th edition ed.) Prentice Hall: Upper Saddle River, New Jersey, 658. ISBN 0-13-149508-9, 1984.

[33] S. Im, N. Srivastava, K. Banerjee, and K. Goodson, “Scaling analysis of multilevel interconnect temperatures for high performance ICs,” IEEE Transactions on Electron Devices, 52(12), pp. 2710–2719, 2005.

[34] Predictive technology model (PTM) [Online], http://ptm.asu.edu/.

[35] S.C. Wong, G.Y. Lee, and D.J. Ma, “Modeling of Interconnect Capacitance, Delay, and Crosstalk in VLSI,” IEEE Trans. Semicond. Manuf, 13(1), pp. 108-11, 2000.

[36] D. Das, and H. Rahaman, “Analysis of Crosstalk in Single- and Multiwalz Carbon Nanotube Interconnects and its Impact on Gate Oxide Reliability,” IEEE Transactions on Nanotechnology, 10(6), pp. 1362-1370, 2011.

[37] Rossi, J.M. Cazeaux, C. Metra, and F. Lombardi, “Modeling crosstalk effects in CNT Bus architectures,” IEEE Transactions on Nanotechnology, 6(2), pp. 133–145, 2007.

[38] B.K. Kaushik, and S. Sarkar S, “Crosstalk analysis for a CMOS gate driven inductively and capacitively coupled interconnects,” Microelectronics Journal, 39:1834–1842, 2008.

[39] R. Dhiman, and R. Chandel, “Design challenges in subthreshold Interconnect circuits: Compact Models and Performance Investigations for Subthreshold Interconnects,” Springer, XIII 2015, 113, p. 45 illus., ISBN: 978-81-322-2131-9.

[40] K. Agarwal, D. Sylvester, and D. Blaauw, “Modeling and analysis of crosstalk noise in coupled RLC interconnects,” IEEE Transactions on Computer Added Design of Integrated circuits and System, 25(5):892–901, 2006.

[41] S.N. Pu, W.Y. Yin, J.F. Mao, and Q.H. Liu, “Crosstalk prediction of single – and double - walled carbon nanotube (SWCNT/DWCNT) bundle interconnects,” IEEE Transactions on Electron Devices, 56(4), pp.560–568, 2009.

[42] M.K. Rai, R. Khanna, and S. Sarkar, “Crosstalk analysis in CNT bundle interconnects for VLSI application,” IEEJ Trans. Electr. Electron. Eng. 9(4), 391–397, 2014.

[43] L. Akbari, and R. Faez, “Crosstalk Stability Analysis in Multilayer Graphene Nanoribbon Interconnects,” © Springer Science+Business Media New York, Circuits Syst Signal Process, 32:2653–2666, 2013, DOI 10.1007/s00034-013-9606-3.

[44] E. Pop, D. Mann, J. Reifenberg, K. Goodson, and H. Dai, “Electro-thermal transport in metallic single-wall carbon nanotubes for interconnect applications,” IEEE Int. Electron Devices Meet., pp. 253–256. 2005.

[45] J. Hone, M. Whitney, C. Piskoti, and A. Zettl, “Thermal conductivity of single-walled carbon nanotubes,” Phys.Rev.B Condens.Matter, 59(4), pp. R2514-R2516, 1999.

[46] P. Kim, L. Shi, A. Majumdar, and P.L. McEuen, “Thermal transport measurements of individual multiwalled carbon nanotubes,” Phys.Rev.Lett., 87(21):215502, 2001.

[47] Balandin, S. Ghosh, W. Bao, I. Calizo, D. Tewldebrham, F. Miao, and C.N. Lau, “Superior thermal conductivity of single-layer graphene,” Nano Lett., 8(3), pp. 902-907, 2008.

[48] Y. Shin, and K.O. Kim, “Analysis of Power Consumption in VLSI Global Interconnects,” IEEE International Symposium on Circuits and System 2005, DOI: 0-7803-8834-8.

LIST OF PUBLICATIONS

S. No.	Author's name	Title	Journal name	Status
1.	Shubham Arora, Mayank Kumar Rai	Temperature Dependent Modeling and Performance Analysis of Coupled MLGNR Interconnects	Microelectronics Reliability	Communicated

ORIGINALITY REPORT-601461027

ORIGINALITY REPORT

24%	2%	23%	5%
SIMILARITY INDEX	INTERNET SOURCES	PUBLICATIONS	STUDENT PAPERS

PRIMARY SOURCES

1	Rai, Mayank Kumar, Brajesh Kumar Kaushik, and Sankar Sarkar. "Thermally aware performance analysis of single-walled carbon nanotube bundle as VLSI interconnects", Journal of Computational Electronics, 2016. Publication	4%
2	Rai, Mayank Kumar, and Sankar Sarkar. "Temperature dependant crosstalk analysis in coupled single-walled carbon nanotube (SWCNT) bundle interconnects : COUPLED SWCNT BUNDLE INTERCONNECTS PERFORMANCE", International Journal of Circuit Theory and Applications, 2014. Publication	3%
3	Submitted to Thapar University, Patiala Student Paper	2%
4	Rai, Mayank Kumar, Ashoke Kumar Chatterjee, Sankar Sarkar, and B. K. Kaushik. "Performance analysis of multilayer graphene nanoribbon (MLGNR) interconnects", Journal of Computational Electronics, 2016. Publication	2%